UNIVERZITA KARLOVA

Přírodovědecká fakulta

Katedra parazitologie

Studijní program: Biologie

Studijní obor: Parazitologie

Bc. Jitka Kučerová

Interakce mezi hydrogenosomy a endoplasmatickým retikulem u *Trichomonas vaginalis*
Interactions between hydrogenosomes and endoplasmic reticulum in *Trichomonas vaginalis*

Diplomová práce

Školitel: prof. RNDr. Jan Tachezy, Ph.D.

Praha, 2019

Prohlášení:

Prohlašuji, že jsem závěrečnou práci zpracovala samostatně a že jsem uvedla všechny použité informační zdroje a literaturu. Tato práce ani její podstatná část nebyla předložena k získání jiného nebo stejného akademického titulu.

V praze 26. 7. 2019

Podpis

Poděkování:

Především bych chtěla poděkovat svému školiteli prof. RNDr. Janu Tachezymu Ph.D. za jeho čas, skvělé vedení, rady i zpětnou vazbu. Neméně bych chtěla poděkovat členům naší laboratoře Jitce Štáfkové, Míše Marcinčíkové, Petru Radovi, Zdeňku Vernerovi, Tami Smutné a Ivanu Hrdému za cenné rady, pozitivní myšlení, a že se na ně mohu obrátit s jakýmkoliv dotazem. Další dík patří mým rodičům, ktetří mě po celou dobu studia podporovali jak finančně, tak psychicky a bez nich bych nikdy tohoto mezníku nedosáhla.

ABSTRACT

Endoplasmic reticulum-mitochondria encounter structure (ERMES) is a protein complex tethering ER and mitochondria. ERMES consists of four core subunits – Mmm1, Mmm2 (Mdm34), Mdm10 and Mdm12. It was first discovered in *Saccharomyces cerevisiae* and most functional information is based on studies of this organism. ERMES affects mitochondrial distribution and morphology, participates in lipid trafficking and is important for homeostasis of the cell. In *Trichomonas vaginalis*, the human urogenital parasite, three genes for putative, highly divergent components of ERMES complex were predicted. However, the cell localization of these proteins and their function is unknown. This thesis is focused on investigation of ERMES components in *T. vaginalis*, their cellular localization, interactions between components and identification of their possible interacting partners.

ABSTRAKT

ERMES je proteinový komplex spojující endoplasmatické retikulum a mitochondrie. Tento komplex se obvykle skládá ze čtyř proteinů – Mmm1, Mmm2 (Mdm34), Mdm10 a Mdm12. Poprvé byl komplex ERMES objeven u organismu *Saccharomyces cerevisiae,* v němž byl také dobře prozkoumán. ERMES zprostředkovává přenos lipidů, podílí se na distribuci a morfologii mitochondria a hraje významnou roli v udržování homeostázy buňky. U lidského parazita urogenitálního traktu *Trichomonas vaginalis* byla přítomnost komplexu ERMES predikována na základě *in silico* analýzy, která ukázala na tři velmi divergentní homology Mmm1, Mmm2 a Mdm12. Cílem této práce je přinést důkazy, zda se opravdu jedná o subjednotky ERMES, jaká je jejich buněčná lokalizace, zda spolu vzájemně interagují a pokusit se zjisit s jakými dalšími proteiny jsou ve vazbě.

1. INTRODUCTION

Trichomonas vaginalis is a cosmopolitan parasitic protist, which belongs to the eukaryotic supergroup Excavata. It was first discovered by Donné in 1836. *T. vaginalis* is the causative agent of human urogenital trichomoniasis. *T. vaginalis* lives in the vagina and urethra of women causing inflammation with itching and a copious white discharge (leukorrhea). Cervix uteri of infected women has in some cases an erythematous, punctate and papilliform appearance (Petrin et al., 1998). Moreover, trichomoniasis is associated with increased risk of adverse pregnancy and HIV infection (Mirmonsef et al., 2012). In men, *T. vaginalis* occurs in the prostate, seminal vesicles and urethra. Trichomoniasis is sexually transmitted disease that accounts to about 150 million new cases annually (Newman et al., 2015).

T. vaginalis is a flagellate that possesses four free flagella and recurrent flagella that forms an undulating membrane. The cytoskeleton includes microtubular pelta, axostyle and striated fiber costa. *T. vaginalis* belongs to phylum Parabasalia, which have a typical structure that connects Golgi apparatus and parabasal fibers together forming a parabasal body (Honigberg et al., 1964). *T. vaginalis* possesses an anaerobic type of mitochondria named hydrogenosomes (Lindmark & Muller, 1973). Unlike mitochondria, hydrogenosomes use exclusively a fermentative pathway for pyruvate metabolism and substrate level phosphorylation for ATP synthesis. Similarly to mitochondria, hydrogenosomes are surrounded by two membranes, although the inner membrane does not form cristae. Hydrogenosomes and mitochondria also share mechanism for Fe/S cluster synthesis (Tachezy et al., 2001) and protein import (Mentel et al., 2008).

ERMES stands for ER-mitochondria encounter structure. It is a crucial protein complex, which participates in the transfer of lipids and proteins from ER to mitochondria (Kornmann et al., 2009), it is involved in mitochondrial dynamics (Youngman et al., 2004), mitochondrial DNA inheritance and mitophagy (Hobbs et al., 2001). In yeast, impaired function of ERMES leads to overall disfunction of mitochondria and consequently to cell death (Burgess et al., 1994; Kornmann et al., 2009). Therefore, ERMES is essential for the correct development and maintenance of mitochondria which sustain homeostasis of the cell.

T. vaginalis has an extensive network of ER around the nucleus and across the cell. This organelle serves as a factory for production of almost all cell's lipids. Therefore, ER could participate by providing membrane lipids for hydrogenosomes.

Although close proximity between ER and hydrogenosomes have been described in studies using electron (Benchimol et al., 1996) and immunofluorescent microscopy (Rada et al., 2019), the functional interaction is not known.

ERMES in *T. vaginalis* was predicted to consist of three highly divergent homologs of Mmm1, Mmm2 and Mdm12. Here we aim to provide evidence that predicted proteins are indeed components of ERMES, what is their cellular localization, whether there are any interactions between ERMES components as well as to attempt identification of other interacting partners.

2. REVIEW OF LITERATURE

2.1 The origin of ERMES

ERMES complex was discovered in fungi *Saccharomyces cerevisiae* by genome-wide mapping of genetic interactions (Kornmann et al., 2009). Initially it was proposed to be a fungal complex, however it is present in several eukaryotic supergroups. ERMES has been be found in Ameobozoa (*Dictyostelium discoideum*, *Polysphondylium pallidum*, *Acanthamoeba castellani*) Apusozoa (*Thecamonas trahens*), Choanozoa (*Capsaspora owczarzaki*, *Sphaeroforma arctica*) and Exacavata (*Trypanosoma brucei*, *Leishmania major*, *Bodo saltans*, *Naegleria gruberi*). On the other hand, ERMES was not found in organisms containing mitosomes such as *Entamoeba histolytica* or *Giardia intestinalis*. Absence of ERMES was also reported in holozoa (metazoa + unicellular relatives) and Diaphoretickes (Wideman et al., 2013). The simplest explanation for the observed distribution of ERMES in eukaryotes is that it arose as an innovation in the ancestor of a monophyletic group containing Excavata, Amoebozoa, and Opisthokonta (Holozoa + Fungi). An alternative to this could be, although slightly less parsimonious that ERMES could have been present in the LECA and then lost in the common ancestor of the Diaphoretickes megaclade. Either scenario places the root of the eukaryotic tree between the Diaphoretickes and all other eukaryotes (Wideman et al., 2013).

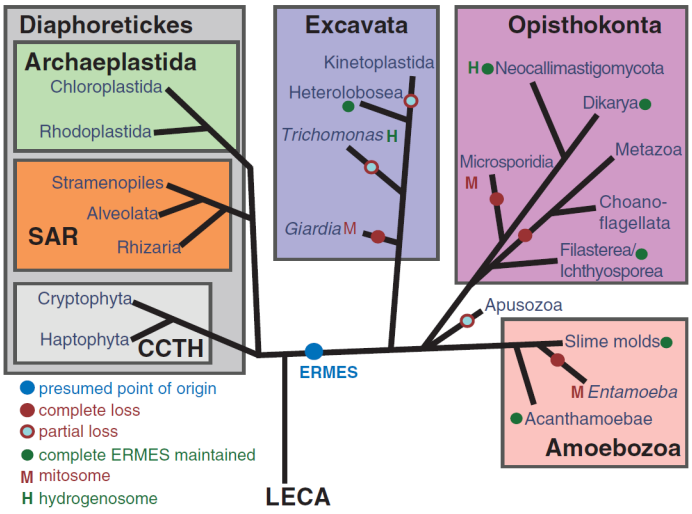

Figure 1. Scheme of evolutionary tree. ERMES was gained by the common ancestor to Excavata, Opisthokonta and Amoebozoa, but lost in the common ancestor of Choanoflagellata and

Metazoa. ERMES has been lost in organisms that have mitosomes (red "M") but maintained in organisms with hydrogenosomes (green "H"). Partial loss of ERMES has been also indicated (Wideman et al., 2013).

Additionally, the fact that ERMES is not present in Archaeplastida and Metazoa suggests that this complex represents potential candidate for drug targeting in animals or plants against Fungi, Ichthyosporea, trypanosomes, Acanthamoeba, Trichomonas, and potentially several other pathogens (Wideman et al., 2013a).

2.2 Components of ERMES

ERMES consists of four structural components: Mmm1 and Mmm2 (syn. Mdm34) (**m**aintenance of **m**itochondrial **m**embrane), Mdm10 and Mdm12 (**m**itochondrial **d**istribution and **m**orphology). The other interacting proteins include Gem1 and Arf1 GTPases which play a role in regulation of ERMES function. ERMES is organized into two to ten foci per cell (Kornmann et al., 2009).

a) Mmm1

Mmm1 protein was first discovered in *S. cerevisiae* (Burgess et al., 1994). This component is located in ER. Disfunction of this protein leads to disintegration of ERMES (Kornmann et al., 2009) and to defect in the transfer of the mitochondrial DNA (mDNA) to daughter cells (Hobbs et al., 2001).

Mmm1 has a transmembrane domain (TMD) located at N terminus, which anchors the protein to the membrane of ER. At the C terminus there is a synaptotagmin-like mitochondrial lipid-binding protein (SMP) domain which is facing the cytosol and directly interacts with Mdm12, the cytosolic bridge. SMP domain of Mmm1 bounds to phospholipids, but preferably to phosphatidylserine (PS), phosphatidic acid (PA), phosphatidylglycerol (PG) and phosphatidylcholine (PC) (Jeong et al. 2016). Mmm1 forms a tightly associated dimer resembling a compact diamond with dimensions of 50 x 60 x 120 Å (Fig. 2). Each subunit forms four helices and six extended and twisted antiparallel β-strands that assemble into typical SMP structure with extended hydrophobic channel for lipid transfer (Jeong et al., 2017).

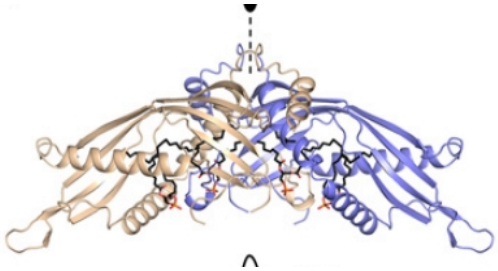

Figure 2. Crystal structure of Mmm1 (Jeong et al., 2017).

b) Mdm12

Mdm12 is a soluble cytosolic protein containing SMP domain that forms a dimer (Fig. 3). Mdm12 monomer forms a β-barrel with incomplete and highly twisted β-strands and three α-helices (Jeong et al., 2016).

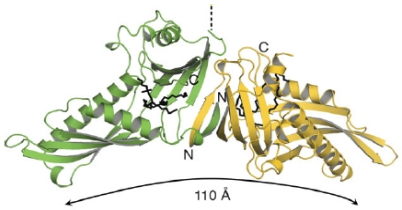

Figure 3. Crystal structure of Mdm12 dimer (Jeong et al., 2016).

Mdm12 has preference for positively charged phospholipids (AhYoung et al., 2015). The protein is essential for normal mitochondrial morphology and inheritance. Defect or loss of Mdm12 results in giant mitochondria and defective transfer of mitochondria to daughter cells (Berger et al., 1997).

Mmm1 and Mdm12 can form a continuous hydrophobic tunnel, which mediates transfer of phospholipids from ER to the mitochondria (Jeong et al., 2017).

c) Mmm2 (syn. Mdm34)

Mmm2 was first identified as an interacting partner to Mmm1 by a genetic screen of mutants (Youngman et al., 2004). Moreover, Mmm2 is allelic with the *mdm34* gene that was also discovered by screen of yeast deletion mutants (Dimmer et al., 2002). Mmm2 is required for the maintenance of mitochondrial shape, mDNA structure and organization.

Mmm2 is usually in discrete foci next to mDNA nucleoids. Mmm1 and Mmm2 partially co-localize (Youngman et al., 2004). However, several studies showed that Mmm1 and Mmm2 do not immunoprecipitate together. Therefore, the association of Mmm2 to Mmm1 is weak or only transient. Nevertheless, Mmm2 is required for normal levels of Mmm1, while Mmm1 is necessary for spotted distribution of Mmm2 (Youngman et al., 2004).

d) Mdm10

Mdm10 is a β-barrel pore-forming protein (Fig. 4) in the mitochondrial outer membrane (MOM) (Sogo et al., 1994), which belongs to porin superfamily together with Tom40 subunit of the outer translocase of MOM (TOM) and Voltage-dependent anion channel VDAC. It exposes long loops towards both sides of the outer membrane (Flinner et al., 2013). Deletion of *mdm10* gene results in mitochondria with altered lipid content (Voss et al., 2012) and changes in mitochondria binding to actin filaments (Boldogh et al., 1998). Moreover, Mdm10 binds to Mmm2 and therefore serves as an anchor to ERMES (Ellenrieder et al., 2016). Another role of Mdm10 is its binding to mitochondrial outer membrane sorting assembly machinery (SAM) to contribute to the release of folded Tom40 from SAM (Ellenrieder et al., 2016). This recent finding contradicts previous thought that Mdm10 has no effect on forming of Tom40 (Flinner et al., 2013).

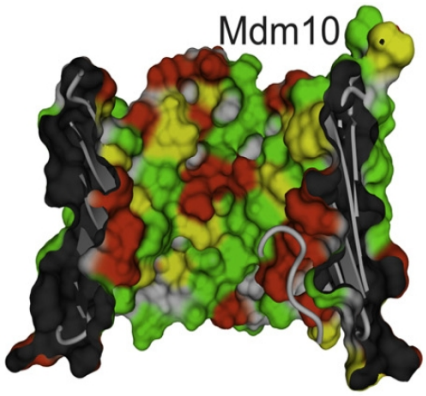

Figure 4. Crystal structure of Mdm10 that was cut open (Flinner et al., 2013).

e) Gem1 and Arf1 GTPases

Gem1 is a genuine subunit of ERMES occurring in smaller quantity, which is not necessary for the assembly of ERMES. Its role is rather regulatory than structural. Gem1 affects the size and number of ERMES complexes in the cell (Kornmann et al., 2011). Other sources report that Gem1 is dependent on higher concentration of calcium to bind to its two EF-hand domains. Gem1 then in return regulates mitochondrial morphology, motility and inheritance (Kornmann et al., 2010).

More recently another GTPase, Arf1, appeared to influence the mitochondrial function (e.g. mitophagy) as well as it was shown that it interacts with Gem1 (Ackema et al., 2014). Cells lacking Arf1 have higher levels of Mmm1 than wild type cells, probably because the deletion of *arf1* gene causes mitochondrial fragmentation and then it would require more ERMES to tether mitochondrial membrane (Zhang et al., 2018).

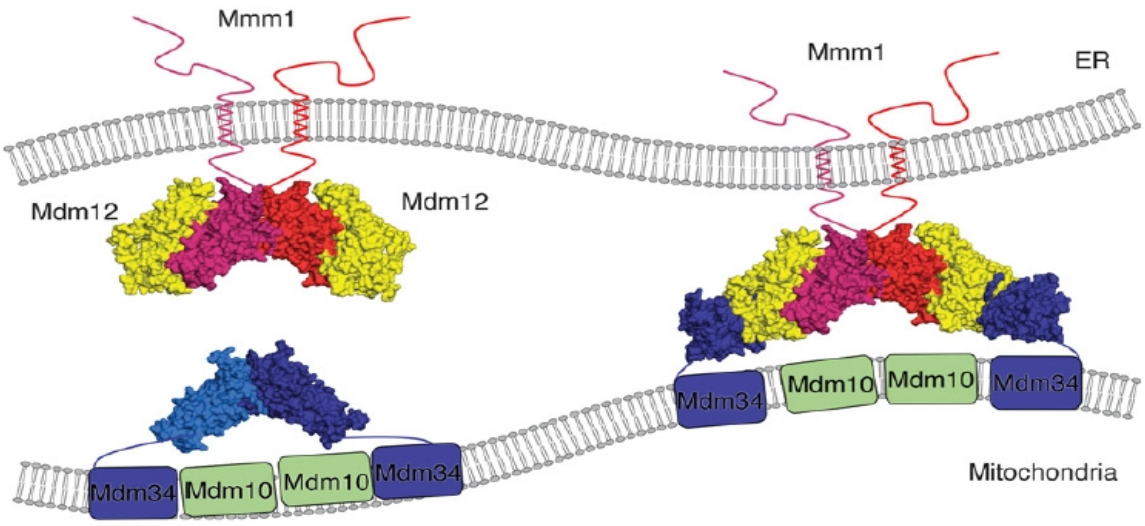

Figure 5. Schematic layout showing the putative organization of the ERMES complex: Mdm12 (yellow); Mmm1 (red); Mmm2 (syn. Mdm34, blue). Mmm1 forms homodimer with a head-to-head contact in the center, capped on each end by a Mdm12 monomer through a tail-to-tail contact. Mdm12 associates with Mmm2 through a head-to-head contact (Jeong et al., 2016).

2.3. The function of ERMES

The communication is a key process of life manifestation on all levels from interactions between humans, via communication among trillion of cells in their organism to intracellular interactions between organelles. Interactions among organelles are the building stones of correctly functioning organism. The most important interactions involve ER and other cellular structures. ER is the largest of membrane-bound organelles within the cell (Lynes et al., 2011). ER can connect to and interact with Golgi apparatus, mitochondria, peroxisomes, endosomes and lysosomes, yet interactions with mitochondria are the most studied connections (Marchi et al., 2014). The proximity of these organelles (10-25 nm) (Csordás et al., 2006) allows them to form ER-mitochondria contact sites (Rowland et al., 2012). These contact sites are referred to as mitochondria-associated membranes (MAM) in mammalian cells (Vance, 1990). In yeast, interactions between mitochondria and ER are executed by the molecular tether ERMES (Kornmann et al., 2009). ER-mitochondria connections are responsible for the biosynthesis of mitochondrial membrane, replication of mitochondrial genome, Ca^{2+} signaling and protein import

(Kornmann et al., 2010). Experimental studies showed that each component of ERMES system is essential and its defect causes diverse mitochondrial phenotypes (Berger et al., 1997).

2.3.1 The phospholipid transfer and assembly

Organelles of endomembrane system including ER, lysosomes, Golgi apparatus, endosomes and plasma membrane are all connected via vesicle trafficking to transport lipids and proteins (Palade, 1975). This is different for organelles of endosymbiotic origin such as mitochondria and chloroplast that gain phospholipids from ER by non-vesicular pathways (Lev, 2010). Close proximity of these organelles might be the advantage for their communication (Helle et al., 2013).

Transfer between mitochondria and ER is essential for membrane biogenesis and for the cell survival. Studies reveal that ERMES not only binds phospholipids but also transfers them from ER to mitochondria. All subunits of ERMES (except for Mdm10) have SMP domains, which are conserved lipid-binding domains found solely in proteins at membrane contact sites (MCS) (Toulmay & Prinz, 2012). Soluble domains of Mmm1, Mmm2 and Mdm12 were purified and experiment demonstrated that they bind phospholipids with the preference for PC. ERMES proteins with SMP domain form an assembly of a three-part complex in which Mdm12 acts like a cytosolic bridge between Mmm1 and Mmm2. This complex may then form a heterohexamer (Fig. 6).

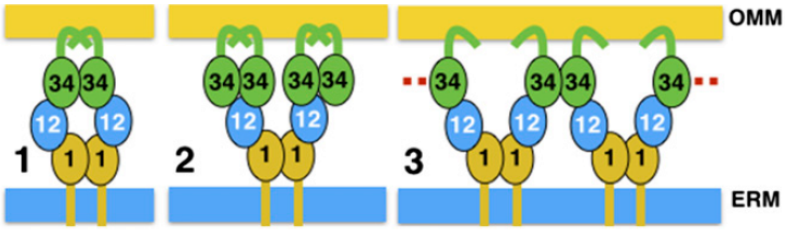

Figure 6. Three plausible models of association among three SMP domains of ERMES (ER to mitochondria contact sites). Mmm2 (34), Mdm12 (12) and Mmm1 (1) (AhYoung et al., 2015).

However, the exact structural model is yet to be elucidated (AhYoung et al., 2015). It has been proposed that ERMES complex transfers phospholipids like a shuffle (Fig. 7) whereas Mmm1, Mdm12, and Mmm2 change their orientations relative to the other components to put the outlet of the lipid-binding pocket of one component close to another component for efficient transfer of lipid molecules. This hypothesis is more likely than ERMES forming one single tunnel (Fig. 8) which assumes presence of one continuous hydrophobic tunnel running from Mmm1 and Mdm12 to Mmm2 for processive movement of lipid molecules (Endo et al., 2018).

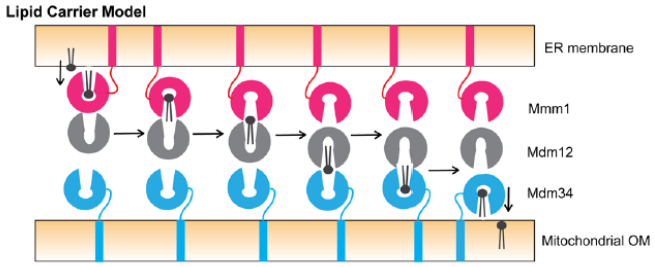

Figure 7. Lipid carrier model (Endo et al., 2018).

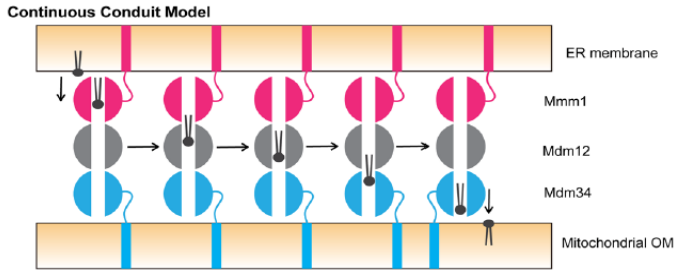

Figure 8. The continuous conduit model (Endo et al., 2018).

The biosynthesis of aminoglycerophospholipids demands intensive exchange of phospholipid precursors between the ER and mitochondria (Tamura et al., 2014). The synthesis of PC in the ER requires transport of PS from the ER to mitochondria to synthesize phosphatidylethanolamine (PE). Then PE is transported back to the ER where PC is synthesized. If one of the ERMES components is compromised, the conversion of PS to PC is disrupted (Kornmann et al., 2009), although other reports showed almost no shift in conversion of phospholipids, apparently due to additional cellular mechanism for phospholipid exchange that can substitute ERMES function (Voss et al., 2012).

2.3.2 ERMES is linked to the organization of mDNA

In yeast, ERMES is organized into two to ten foci per cell (Kornmann et al., 2009) that often co-localize with mitochondrial nucleoids (Hobbs et al., 2001). Nucleoids are nucleoprotein units of mDNA which are engaged in replication of mDNA (Nass, 1969). It seems that Mmm1 and Mmm2 play role in the regulation of mDNA nucleoid structure. Deletion of any one of the ERMES subunits results in loss of mDNA organization (Youngman et al., 2004) and in loss of mDNA (Boldogh et al., 2003). Since mDNA is attached to the mitochodrial membrane at discrete foci (Miyakawa et al., 1987), disruption of nucleoid structure maybe due to the loss of attachment to the membrane (Youngman et al., 2004). Defect in nucleoid maintenance affects mitochondrial motility. Mitochondria without mDNA move 2-3 times faster than mitochondria with mDNA (Boldogh et al., 2003). Deletion of any component has also negative effect on morphology of mitochondria that form large, spherical structures (Fig. 9) (Burgess et al., 1994) (Boldogh et al., 1998).

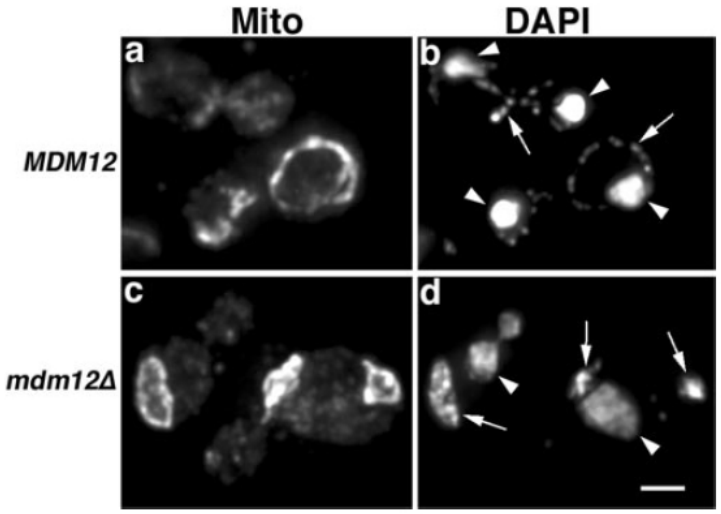

Figure 9. Defects in mtDNA nucleoid stability in cells with impaired Mdm12 protein. Cells are visualized with IF microscopy. MDM12 – wild type (a and b). Mutants mdm12Δ (c and d) show enlarged mitochondria. Fixed cells were stained with anti-mitochondrial antibody (a and c). mtDNA was visualized using DAPI (b and d) (Boldogh et al., 2003).

2.3.3 ER-mitochondria junction required for iron homeostasis

Additional role of ERMES is regulation of iron homeostasis. Disruption of ERMES function causes inappropriate induction of the iron deficiency response and accumulation of iron inside the cell (Xue et al., 2017). Iron is an essential element for numerous biochemical pathways in the cell - the most important is the biosynthesis of iron-sulfur clusters which are cofactors of many fundamental proteins (Stehling et al., 2013). Studies suggest that regulation function of ERMES in iron homeostasis can be bypassed without restoring ER-mitochondria junctions, indicating that functional communication is more important than the physical connection between the ER and mitochondria (Xue et al., 2017).

2.3.4 ERMES complex is essential for actin-dependent mitochondrial motility

Mmm1, Mdm10 and Mdm12 proteins are required to link mitochondria to actin cables for linear, polarized movement (Boldogh et al., 2003). Mutations in any of these proteins result in accumulation of abnormal, spherical mitochondria and defects in mitochondrial distribution, actin association and motility (Boldogh et al., 2003). Nevertheless, other sources report that defects in mitochondrial inheritance are a secondary consequence of a morphology change. Abnormally shaped mitochondria were transported to new buds despite the absence of ERMES components, apparently due to overexpression of inheritance-promoting factor Ypt11 (Nguyen et al., 2012).

3. THE AIMS OF THE THESES

The overall goal of the theses was to provide evidence about the presence of ERMES complex in *T. vaginalis*.

Specific aims:

1) To express tagged version of predicted ERMES components Mmm1, Mmm2 and Mdm12 in *Trichomonas vaginalis* and to investigate their cellular localization using super-resolution microscopy and cell fractionation.
2) To express different combinations of ERMES components using double transfection of *T. vaginalis* and to investigate interactions between these components using super-resolution microscopy.
3) To investigate interactions between ERMES components and to identify new interacting components using immunoprecipitation of protein complexes and label-free mass spectrometry.

4. MATERIAS AND METHODS

4.1. Cultivation

4.1.1 Cultivation of *Trichomonas vaginalis*

T. vaginalis strain TvT1 was obtained from J. H. Tai (Institute of Biomedical Sciences, Taipei, Taiwan). Trichomonads were cultivated in modified Diamond's Trypton-Yeast extract-Maltose (TYM) medium, supplemented with 10 % horse inactivated serum and adjusted to pH 6.2 (Diamond, 1957) at 37 °C.

Modified Diamond's TYM medium 6.2	
Tryptone (OXOID)	20 g
Yeast extract (OXOID)	10 g
Maltose (Sigma)	5 g
K_2HPO_4 (Sigma)	0,8 g
KH_2PO_4 (Sigma)	0,8 g
L-Cysteine (Sigma)	1 g
Ascorbic acid (Sigma)	0,2 g
Ammonium iron (III) citrate (Sigma)	22,8 mg
Distilled H_2O	900 ml
Inactivated horse serum (Gibco® Life technologies)	100 ml

- when all the components are dissolved in the water, adjust pH to 6,2 with 1M HCl
- fill the medium to bottles and autoclave for 25 minutes at 120 °C and the pressure 120 kPa
- add the horse serum when the medium is cooled down
- store at 4 °C for two weeks or at -20 °C for longer period of time

- for transfection experiments, supplement medium with antibiotics:

G418 (ZellBio GmbH)	100 mg/ml
Puromycin (ZellBio GmbH)	200 mg/1ml

4.1.2 Cultivation od *Escherichia coli*

TOP10 strain of *Escherichia coli* (Thermofisher) was used for plasmid propagation. *E. coli* strain was incubated in Luria-Bertani (LB) medium (Bertani, 1951) at 37 °C on the shaker (220 rpm). Transformed cells were cultured on LB plates with agar and selective antibiotics according to type of vector - Ampicillin (Sigma) (100µg/ml) or Kanamycin (50µg/ml).
Storage of *E. coli* at -80 °C: glycerol of 20 % final concentration can be added into LB medium.

Cultivation media for *E. coli*:

LB medium:

LB medium (Sigma)	20 g
Distilled H_2O	500 ml
store at 4 °C	

LB agar plates:

LB agar (Sigma)	17 g
Distilled H_2O	500 ml

SOC medium (pH 7):

Tryptone (Sigma)	2 g
Yeast extract (Sigma)	0,5 g
NaCl (Sigma)	0,058 g
250 mM KCl (Sigma)	1 ml
Distilled H_2O	100 ml

- after sterilization add:

Glucose (20 %) sterile (Sigma)	1,8 ml
2 M $MgCl_2$ (Sigma)	0,5 ml

- medium is stored at -20 °C

Antibiotics:

Ampicillin (Sigma):	100 mg/ml

4.2. Buffers and solutions

4.2.1 DNA fragment cloning

Buffer for DNA electrophoresis (Ogden & Adams, 1987):

10X Tris-Acetate-EDTA (TAE) (Bio-Rad)	100 ml
Distilled H_2O	900 ml

DNA staining dye:

SYBR®Safe DNA gel stain (ThermoFisher)

Agarose gel 1 %:

Agarose (Serva)	40 mg
1xTris-Acetate-EDTA (TAE) (Bio-rad)	40 ml
SYBR®Safe DNA gel stain (ThermoFisher)	40µl

4.2.2 Protein analysis

Sodium Dodecyl Sulphate-Polyacrylamide Gel Electrophoresis **(SDS-PAGE) gel:**

(for 12 % 0,75 mm thick acrylamide hand-cast mini gel, appropriate gel percentage based on protein size, 12% is optimal for proteins ranging from 10 to 70 kDa)

30 % Acrylamide/Bis solution (Bio-Rad)	1,36 ml
C solution	2 ml
TEMED (Tetramethylethylenediamine)	5 µl
G solution	40 µl
Distilled H_2O	0,64 ml

SDS-PAGE stacking gel (5 %)

30 % Acrylamide/Bis solution (Bio-Rad)	0,24 ml
D solution	0,75 ml
TEMED	5 µl
G solution	20 µl
Distilled H_2O	0,47 ml

C solution:

TRIS (Sigma) adjust pH to 8,8	9,1 g
SDS	0,2 g
Distilled H_2O	add to final volume of 100 ml

- store at 4 °C

D solution:

TRIS (Sigma) pH 6,8	3 g
SDS	0,2 g
Distilled H_2O	add to final volume of 100 ml

- store at 4 °C

G solution:

Ammonium persulfate (Sigma)	1 g

- dissolve in 10 ml of H_2O, prepare aliquots, store at -20 °C

SDS-PAGE buffer:

10X Tris-Glycine-SDS (TGS) (Biorad)	100 ml
Distilled H_2O	900 ml

4.2.3 Western blot analysis

Blotting buffer:

10X concentrated SDS (TGS) buffer (Biorad)	100 ml
Methanol (Lach-Ner)	200 ml
Distilled H_2O	700 ml

Blocking buffer (5 %):

1x nonsterile phosphate buffered saline (PBS)	300 ml
Dried skim milk (Nutristar)	15 g
Tween 20 (Sigma)	150 µl

10X PBS:

NaCl (Sigma)	80 g
KCl (Sigma)	2 g
$NaH_2PO_4 \cdot 12\ H_2O$ (Sigma)	14,4 g
KH_2PO_4 (Sigma)	2,4 g

- adjust pH to 7,4

Distilled H_2O	fill volume to 1 l

Ponceau S:

Ponceau S (Merck) (final concentration 0,5 %)	38 g
Acetic acid (Lach-Ner) (final concentration 1 %)	1 ml
Distilled H_2O	fill volume to 100 ml

Substrate for alkaline phosphatase:

Sigma Fast BCIP/NBT tablet	1 piece
Distilled H_2O	10 ml

Substrate for horseradish peroxidase:

Western HRP substrate Forte (Merck)	1ml per membrane
Western HRP substrate Classico (Merck)	1ml per membrane

4.2.4 Isolation buffers and solutions

Sacharose-Tris (ST) isolation buffer (pH 7,2):

Sacharose (Sigma)	42,85 g
TRIS (Sigma)	0,6 g
KCl (Sigma)	18,5 mg

- adjust pH to 7,2

Distilled H_2O	add to final volume of 500 ml

- store at -20 °C

2X Immunoprecipitation (IP) buffer:

TRIS (Sigma) 100 mM (final pH 7,2-7,4)	3,03 g
NaCl (Sigma) 300 mM	4,38 g
Distilled H_2O	250 ml

IP wash buffer:

2X IP buffer	5 ml
Triton X-100	0,05 % final concentration
Distilled H_2O	4,95 ml

Protease inhibitors:

Stock solution:	
Tosyl-L-lysine-chlormethylketone (TLCK) (Sigma)	25 mg/ml
Leupeptin (Sigma)	5 mg/ml
Complete tablets (Roche)	1 tablet/ 50 ml of IP buffer

4.2.5 Buffers for immunofluorescence microscopy

2x PEM buffer (pH 6,9) (Mooberry et al., 1999):

PIPES (Sigma)	30,2 g
0,5 mM EGTA (Sigma)	2 ml
1M $MgSO_4$ (Sigma)	100 µl

- keep on adding 1M NaOH until the solution gets transparent, then adjust pH to 6,9 and add distilled H_2O to final volume of 500 ml, this solution needs to be autoclaved

PEMBALG:

1x PEM buffer	100 ml
Bovine Serum Albumin (BSA)[1] (Sigma)	1 g
Lysine (Sigma)	1,8 g
Coldwater fish skin gelatin (Sigma)	0,5 g

4.2.6 Antibodies

Primary antibodies:

Anti-HA monoclonal antibody (mouse IgG) (Exbio) (working dilution 1:400 for western blot, 1:1000 for immunofluorescence microscopy)

Anti-V5 monoclonal antibody (rabbit IgG) (Abcam) (working dilution 1:1000)

Rabbit polyclonal anti malic enzyme (*T. vaginalis*) antibody (working dilution 1:500)

Rabbit polyclonal anti β subunit of succinate-CoA ligase (SCS) antibody (*T. vaginalis*) (working dilution 1:1000)

Rabbit polyclonal anti C-tail protein CTA10 (TVAG_277930) antibody (working dilution 1:100)

Secondary antibodies:

Anti-mouse IgG antibody coupled with alkaline phosphatase produced in goat (ICN/CAPPEL) (working dilution 1:2000)

Anti-rabbit IgG antibody coupled with alkaline phosphatase produced in goat (ICN/CAPPEL) (working dilution 1:2000)

Anti-mouse IgG antibody coupled with horseradish peroxidase produced in goat (Novex ECL) (working dilution 1:2000)

Anti-rabbit IgG antibody coupled with horseradish peroxidase produced in goat (Novex ECL) (working dilution 1:2000)

Alexa Fluor 594 donkey anti mouse antibody (ThermoFisher) (working dilution 1:1000)

[1] heat shock fraction, protease free, pH 7

Alexa Fluor 594 donkey anti rabbit antibody (ThermoFisher) (working dilution 1:1000)
Alexa Fluor 488 donkey anti mouse antibody (ThermoFisher) (working dilution 1:1000)
Alexa Fluor 488 donkey anti rabbit antibody (ThermoFisher) (working dilution 1:1000)

4.3. Methods

4.3.1. Gene cloning

4.3.1.1 Design of primers

Geneious 8.0 was used for the design of primers based on following criteria:

- primers have the length of 18–30 nucleotides
- optimal melting temperature (Tm) of the primers is between 52 °C and 70 °C and within 5 °C difference from each other, the higher the Tm the more specific the binging is
- if the Tm of primer is lower than 52 °C, find more GC rich sequence, or extend the length of the primer
- aim for the GC content to be between 40 and 60 %, with C or G at the 3' end of a primer to promote binding
- have a balanced distribution of GC-rich and AT-rich domains
- avoid runs of one nucleotide or dinucleotide repeats
- if the primers are used for mutagenesis, have the mismatched bases towards the middle of the primer

Table 1. List of designed primers.

***mmm1* TVAG_214860**	
forward, **NdeI**	5'-**CATATG**AAACATATTGATATTGGATT-3'
reverse, **BamHI**	5'-**GGATCC**AGCTTGTGGAATTTTAATTTCTATC-3'
annealing 57 °C	
***mmm2a* TVAG_217400**	
forward, **NdeI**	5'-**CATATG**TCTCTACAATTTGATTGGGAG-3'
reverse, **BamHI**	5'-**GGATCC**AGAAATTCAAATTCCACAAACT-3'
annealing 64 °C	
***mmm2b* TVAG_375920**	
forward, **NdeI**	5'-**CATATG**ATGTCTCTACAGTTTGATTGGGAGG-3'
reverse, **BamHI**	5'-**GGATCC**AGCTTGTGGAATTTTAATTTCTATCTTAGG-3'
annealing 69 °C	
***mdm12* TVAG_063000**	
forward, **NdeI**	5'-**CATATG**TCATTACGCTTAACTGGGA-3'
reverse, **BamHI**	5'-**GGATCC**CTGGGTAGGCTGATTGAATGG-3'
annealing 65 °C	

Primers were produced by Sigma-Aldrich.

4.3.1.2 Amplification of genes

Genes for ERMES components were amplified by polymerase chain reaction (PCR). Genomic DNA (gDNA) isolated from *T. vaginalis* T1 strain was used as a template. gDNA was isolated using Genomic DNA Mini Kit (Geneaid).

PCR reaction protocol:

volume of reaction 25 µl

Q5® High-Fidelity DNA polymerase (New England Biolabs)	0,25 µl
Q5 polymerase buffer	5 µl
Forward primer 10 µM	1,25 µl
Reverse primer 10 µM	1,25 µl
dNTP (Thermofisher) 10 mM	0,5 µl
gDNA (1ng - lµg)	0,5 µl
MiliQ sterile H_2O	16,25µl

Thermocycler settings:

STEP	TEMPERATURE	TIME
Initial Denaturation	98°C	30 seconds
30 Cycles	98°C	10 seconds
	50–70°C*	10–30 seconds
	72°C	20–30 seconds/kb
Final Extension	72°C	3 minutes
Hold	4°C	∞

*calculate annealing temperature of primers for the best results

- PCR reaction can be stored at -20 °C or immediately used for further experiments

DNA electrophoresis and purification:

- load mix of PCR reaction with loading dye in the ratio 1:6 on 1 % agarose gel
- to estimate length of PCR product, use ladder GeneRuler™ (BIOGEN)
- run electrophoresis at 100 V for 30 minutes
- place gel under UV transilluminator and cut out band of expected size, then purify the PCR product with Gel/PCR DNA Fragments Extraction Kit (Geneaid)

Ligation of PCR product into pJET1.2/blunt:

pJET1.2/blunt vector (Fig. 10) was used for cloning of PCR products.

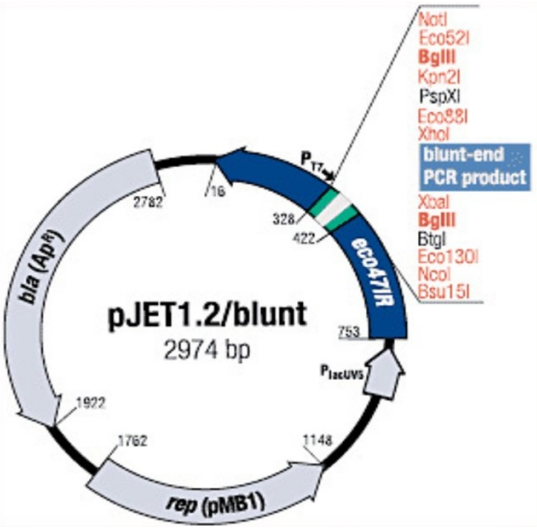

Figure 10. pJET1.2/blunt Vector Map (CloneJET PCR Cloning Kit - Thermo Fisher Scientific)

Cloning sites: NdeI, BamHI

Resistance: ampicillin

Ligation protocol:

volume of reaction 10 µl

pJET1.2/blunt vector:	0,5 µl
T4 DNA ligase:	0,5 µl
PCR product:	4 µl
Buffer:	5 µl

- leave 30 minutes at room temperature (RT)

***E. coli* (TOP 10) transformation protocol:**

- take aliquot (150 µl) of *E. coli* TOP 10 competent cells out of -80 °C and place it on ice for 10 minutes
- add plasmid (10 µl) and incubate the cells with vector for 20 minutes on ice
- in the meantime, thaw SOC medium and preheat LB agar plates at 37 °C
- after incubation perform heats hock by incubating cells for 30 seconds at 42 °C in water bath

- place cells on ice for 2 minutes
- after incubation add 250 µl of SOC
- place cells on shaker for 1 hour at 37 °C using 22 RPM shaking
- add 50 µl of antibiotics and 30 µl of culture on LB agar plates and distribute with sterile glass beads
- incubate plates with bacteria overnight (preferably 16 hours) at 37 °C
- for storage place at 4 °C and protect against water precipitation

Plasmid Mini-prep preparation:

- colonies of transformed bacteria grew overnight on plates, pick few candidates colonies with a tip and inoculate into 5 ml of LB medium with antibiotics (5µl of stock solution) and incubate overnight at 37 °C in the shaker
- harvest cells on 8000 x g at 4 °C for 10 minutes and isolate plasmid with miniprep kit (High-Speed Plasmid Mini Kit by Geneaid) according to the manufacturer protocol
- measure concentration of isolated plasmid with NanoDrop™ 2000 Microvolume Spectrophotometer (ThermoFisher) (mini-prep should have 600-800 ng of DNA per µl) and submit sample for sequencing to verify correct sequence of the insert

Sequencing sample:

1 µl plasmid (concentration 600 ng/µl) + 0,5 µl 10µM primer + 6,5 H_2O

Gene cloning to TagVag2 vector:

To re-clone a gene of interest from pJET1.2/blunt to TagVag2, both vectors were restricted at NdeI and BamHI sites.

TagVag2 is a vector for expressing proteins in *T. vaginalis* (Hrdy et al., 2004). Proteins are expressed under α-subunit of succinyl-coenzyme A (CoA) synthetase (SCS) gene promoter. TagVag2 sequence (Fig. 11) encodes genes for ampicillin and geneticin (or puromycin - Fig. 12) resistance and influenza hemagglutinin (HA) tag. Vector without insert is about 5000 bases long.

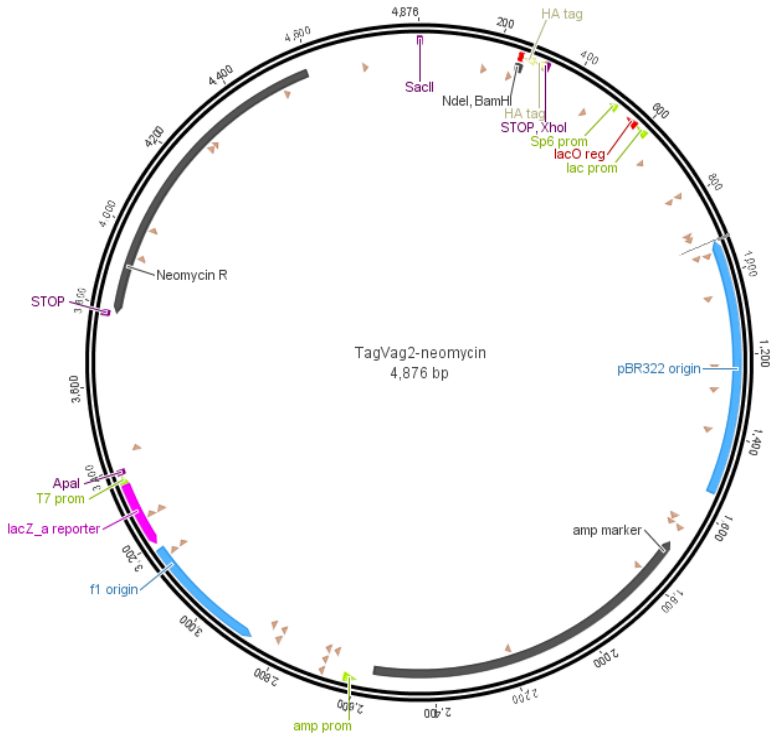

Figure 11. The sequence of TagVag2 expression plasmid with encoded geneticin resistance (Hrdy et al., 2004).

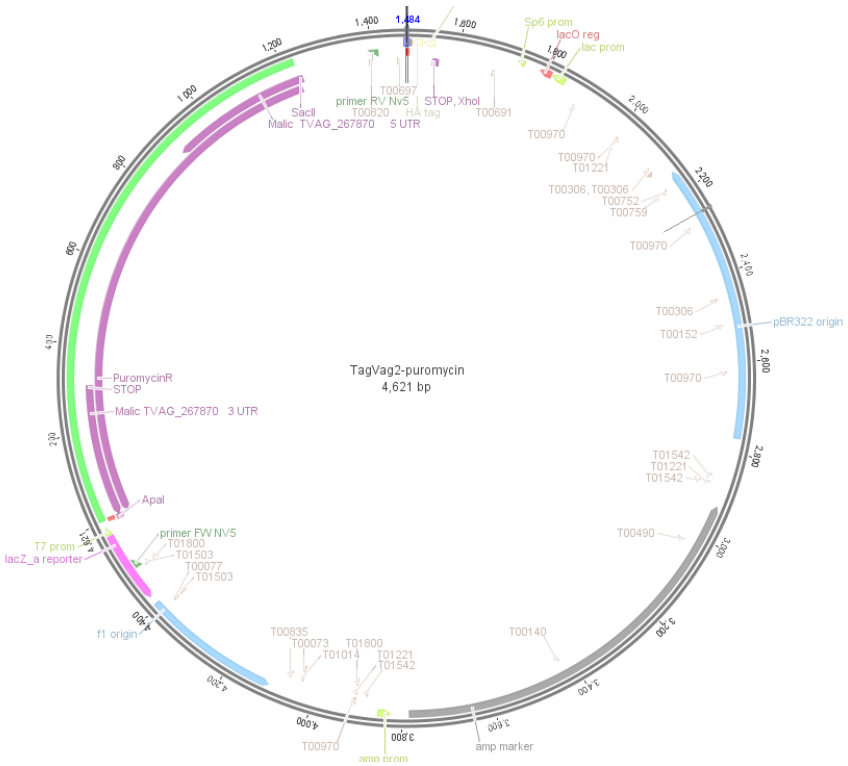

Figure 12. The sequence of TagVag2 expression plasmid with encoded puromycin resistance (Hrdy et al., 2004).

Restriction protocol:

- use FastDigest Green Buffer (10X)

NdeI (Thermofisher)	1 µl
BamHI (Thermofisher)	1 µl
Fast digest buffer	2 µl
Vector (0,5-1 µg/ µl)	2 µl
Sterile H_2O	14 µl

- mix gently and incubate for 5-15 minutes at 37 °C
- after incubation analyze samples with DNA electrophoresis, cut out bands corresponding to backbone of TagVag2 and to insert from pJET1.2/blunt and elute DNA from the gel with Gel/ PCR DNA Fragments Extraction Kit (Geneaid)
- ligate linearized Tagvag2 and insert (gene of interest sequence) according to following equation:

{ [ng of vector] x [kb size of insert] } / { kb size of vector } x (insert:vector ratio) = ng of insert required

Ligation protocol:

final volume 10 µl

x µl of donor plasmid + y µl insert + 1 µl T4 DNA ligase + 1 µl T4 DNA ligase buffer

- ligate overnight at 4 °C
- transform bacteria TOP10 with this mixture according to the transformation protocol, isolate TagVag2 plasmid and verify correct ligation by sequencing as above

Mutagenesis of Mmm1 (TVAG_214860) **and Mdm12 (**TVAG_063000)

Coding sequences of genes (TVAG_063000 and TVAG_214860) contain restriction site for NdeI. Therefore, before cloning to the TagVag2 vector, the restriction sites were erased by mutagenesis using PCR. We performed this mutagenesis using Q5® Site-Directed Mutagenesis Kit (New Englad Biolabs®). This kit is designed for rapid and efficient incorporation of insertions, deletions and substitutions into double-stranded plasmid DNA. The first step involves PCR using mutagenesis primers (Fig. 13). The second step involves incubation with enzyme mix containing a kinase, a ligase and DpnI. Together, these enzymes allow circularization of the PCR product and removal of the template DNA.

Mutagenesis primers designed by http://nebasechanger.neb.com/ server:

Table 2. List of mutagenesis primers.

***mmm1* TVAG_214860**	
Forward	5'-TTTCCTTCCACATGAAAGTAGAATTAATTTTATG-3'
Reverse	5'-ATAGCTGTGGTATATCAATTG-3'
annealing 57 °C	
***mdm12* TVAG_063000**	
Forward	5'-CATTACAGTCTTATGTAGTTCAAGAAAG-3'
Reverse	5'-CATCCCAGTTAATGCGTAATG-3'
annealing 62 °C	

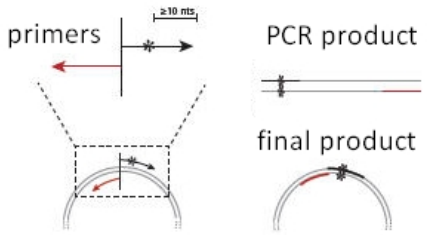

Figure 13. Schema of mutagenesis during PCR (New England Biolabs).

Mutagenesis reaction protocol:

- 1st STEP: PCR reaction (volume 25 µl):

Q5® High-Fidelity DNA polymerase	0,25 µl
Q5 buffer	5 µl
dNTP	0,5 µl
Mutagenesis primer FW	1,25 µl
Mutagenesis primer RV	1,25 µl
Plasmid[2]	(1-25 ng)
Nuclease free H_2O	fill to 25 µl

- mix reagents and proceed with PCR

- 2nd STEP: Kinase, Ligase & DpnI (KLD) Treatment:

Mix the following reagents:

PCR reaction	1 µl
2X KLD Reaction buffer	5 µl
10X KLD Enzyme mix	1 µl
Nuclease free H_2O	3 µl

- incubate at RT for 5 minutes then proceed with standard transformation protocol, then proceed with miniprep and perform sequencing on isolated plasmids

[2] plasmid pJET 1.2 blunt with subcloned gene that still has non-mutated sequence

4.3.2 Selectable transformation of *T. vaginalis*

Transformation of *T. vaginalis* based on electroporation is performed using modified methods of Delgadillo (Delgadillo et al., 1997). The transformation requires around 1000-1500 ng of TagVag2 plasmid per µl that was obtained using Plus Midipreps DNA Purification System (Wizard®) according to manufacturer protocol. DNA concentration was measured using NanoDrop™ 2000 Microvolume Spectrophotometer (ThermoFisher).

Transfection protocol:

- harvest 500 ml of T1 culture in logarithmic phase of growth in 50 ml sterile falcon tubes by centrifugation (1000 x g, for 15 minutes, at 4 °C)
- weigh pellet of cells and resuspend it in 0,5 ml of TYM media per 1 g of trichomonads
- pass cell suspension two times through 23G needle
- place 0,4 cm Gene Pulser cuvette on ice and add 300 µl of cell suspension and 30-50 µl of plasmid (concentration 0,7-1 µg/µl)
- gently resuspend and incubate on ice for 10 minutes
- use Exponential protocol (350 V/975 nF) for electroporation by Gene Pulser (BioRad)
- place electroporated cells immediately in preheated TYM 6,2 media with antibiotics Penicillin-Streptomycin 1000 U/ml (Gibco™) and incubate at 37 °C
- after 6 hours add selective antibiotic (G418 or puromycin) in concentration of 200 µg/ml
- check electroporated cells daily, growth is visible after 3-10 days

4.3.3 SDS page

- dissolve protein samples in SDS buffer and boil at 95 °C for 5 minutes then load samples on 12 % polyacrylamide gel with SDS

- for the determination of molecular weight use PageRuler™ Plus Prestained Protein Ladder (ThermoFisher)
- run gel in Mini-PROTEAN® Tetra Vertical Electrophoresis Cell for Mini Precast Gels (BioRad) at 50 V for samples to reach the lower gel, then increase voltage to 180 V, run gel until the sample dye is approximately 1 cm above the bottom of the gel
- remove glass and cut off the stacking gel
- analyze gel by Western blotting (WB), staining with Brilliant Blue, etc.

4.3.4 WB analysis

- soak 5,5 x 8,5 cm nitrocellulose blotting membrane Amersham™Protran™ 0,2 µm NC (GE Healthcare Life science) and two pieces of Western blotting filter paper (1 mm thick) in the blotting buffer
- stack components on the semi-dry blotting device FASTBLOT™ (Biometra) in the order: filter paper, membrane, gel, filter paper
- perform protein transfer to nitrocellulose membrane for an hour at 3 mA per cm^2 of membrane
- stain membrane with Ponceau S to check whether the protein transfer was successful
- stop staining with distilled H_2O
- place blot to the blocking buffer for an hour at RT or overnight at 4 °C
- then add primary antibody in blocking buffer to the membrane and incubate for 1 hour or overnight at 4 °C
- wash membrane three times with blocking buffer for 10 minutes
- after washing add secondary antibody in blocking buffer to the membrane and incubate for an hour at RT
- after incubation wash membrane two times with PBS + 0,1 % Tween for 5 minutes and then two times with PBS for 10 minutes
- incubate membrane with the substrate for horseradish peroxidase (for chemiluminescence) or alkaline phosphatase

- when choosing horseradish peroxidase, use Amersham Imager 600 for analyzing the membrane

4.3.5 Preparation of slides for immunofluorescence microscopy

- take 8 ml of trichomonas culture and add formaldehyde (2 % final concentration), incubate at 37°C for 30 minutes
- after incubation with formaldehyde spin culture on 900 x g at RT for 5 minutes
- resuspend pellet in 5 ml of PEM and spin on 900 x g at RT for 5 minutes
- gently resuspend pellet in 160 µl of PEM and form drop on the cover glass (170 µm thick, ZEISS, that was cleaned with 96 % ethanol and treated with poly-lysine), then gently disperse the drop across the cover glass
- let dry for 20 minutes, aspirate the excess culture
- add 0,1 % Triton X-100 in PEM on the cover glass for 25-minute permeabilization
- after permeabilization carefully aspirate slides and wash with PEM three times for 5 minutes
- after washing add PEMBALG and incubate slides for 60 minutes
- add primary antibody in PEMBALG and incubate for 60 minutes
- after incubation wash slides three times for 10 minutes
- add secondary antibody in PEMBALG and incubate for 60 minutes
- wash slides three times for 10 minutes and then mount them using antifade mounting medium Vectashield® (Vector) with 4′,6-diamidine-2′-phenylindole dihydrochloride (DAPI) onto StarFrost® microscope slides
- seal cover slide with nail polish
- use Nikon N-SIM with software NIS-Elements Ar (v4.60) to analyze slides
- edit pictures with Image J software

4.3.6 Cell fractionation by differential centrifugation

- harvest 250-500 ml of trichomonas culture on 1000 x g at 4 °C for 15 minutes
- wash pellet of cells with ST buffer and spin on 1000 x g at 4 °C for 15 minutes

- resuspend pellet in 40 ml of ST buffer with inhibitors of proteases (Leupeptine, TLCK – 0,2 % final concentration)
- sonicate cell suspension (on ice) with 1-sec pulses, 1-minute intervals with amplitude 40 % until approximately 95 % of cells are broken
- spin homogenate at 800 x g for 20 minutes to remove unbroken cells and cell debris
- transfer supernatant into 26,3 ml polycarbonate centrifugation tubes and spin on 13 500 RPM at 4 °C for 20 minutes (in VTi-70 rotor)
- aspire supernatant and spin it on 100 000 x g at 4 °C for 30 minutes to obtain cytosolic fraction
- resuspend pellet that contains hydrogenosomes and low-density vesicles (LDV) in 1 ml of ST buffer (large granular fraction, LGF)

Isolation of hydrogenosomes:

- spin LGF in 1 ml of ST buffer with inhibitors on 13 500 RPM at 4 °C for 10 minutes in small 1,5 ml eppendorf tubes
- aspire supernatant and also white sediment of LDV, resuspend hydrogenosomes in 1 ml of ST buffer with inhibitors and spin on 13 500 RPM at 4 °C for 10 minutes, repeat this step until you get pure hydrogenosomal fraction

4.3.7 Purification of hydrogenosomes using Percoll gradient

Prepare Percoll solution:

2 x ST buffer	18 ml
Percoll® (Sigma)	16,2 ml
H_2O	1,8 ml
(TLCK and Leupeptin)	each 72 µl (0,2 % final concentration)

- mix in 36,2 ml Optiseal tube (Beckman) by inverting the tube several times
- remove about 3 ml of solution from the tube and add resuspended LGF in 1ml of ST

- add ST with Percoll to remove any bubbles, insert the lid and cover with cap, then invert carefully several times
- spin at 30 000 RPM (in VTi-50 rotor) for 35 minutes at 4 °C with low brake (ultracentrifuge Optima XE, Beckman, deceleration 9)
- hydrogenosomes appear as a lower, darker band, LDV is less dense and lighter
- first, take LDV and then aspire the solution until you reach hydrogenosomes
- remove hydrogenosomes using pipette, both LDV and hydrogenosomes need to be washed in ST buffer and spinned in polycarbonate tubes at 13 500 RPM (rotor VTi-70) for 20 minutes at 4 °C to remove Percoll

4.3.8 Determination of latency of malic enzyme (ME) activity

To check the quality of purified hydrogenosomes, the latency of ME, which is the marker for hydrogenosomal matrix, is determined:

Reaction mixture:

ST buffer	2 ml
100 mM β-NAD	20 µl
0,5 M L-malate disodium salt	40 µl
10 % Triton X-100	5 µl
Hydrogenosome sample	5 µl

- mix ST buffer and malate in the cuvette and start the reaction by adding NAD
- measure NAD reduction for about 30 seconds (this is the free activity), then add Triton X-100 and continue monitoring
- latency is defined as a difference between free ME activity (without Triton X-100) and total activity after addition of the detergent
- latency should be at least 90%

4.3.9 Protease protection assay

This method was used to establish the topology of hydrogenosomal protein Mmm2. Proteinase K is a broad-spectrum serine protease and digests only proteins that are not protected by membranes. For control we used SCS, which is hydrogenosomal matrix protein protected by hydrogenosomal membranes and C-tail anchored protein CTA10, which is outer hydrogenosomal membrane protein.

- harvest hydrogenosomes and measure the protein content with Bicinchoninic Acid protein determination kit (Sigma)
- measure latency of ME, which should be at least 90 %
- split hydrogenosomes into three samples (each having 1-10 mg of protein in 50µl of ST buffer)
- sample 1 serves as a control
- add proteinase K (Roche; 50µg/ml final concentration) to the sample 2 and incubate on ice for 30 minutes, stop reaction with phenylmethylsulfonyl fluoride (PMSF) of 2 mM, spin sample on 15 000 x g at 4 °C for 5 minutes and resuspend pellet in SDS buffer and boil for 5 minutes
- pre-incubate sample 3 with Triton X-100 (1 % final concentration) for 10 minutes then add proteinase K (50µg/ml final concentration) and incubate on ice for 30 minutes, stop reaction with PMSF of 2 mM
- spin sample at 15 000 x g at 4 °C for 5 minutes
- follow with **Chloroform-methanol extraction protocol** (for sample 3)**:**
- take supernatant, add methanol in the ratio 1:1 and vortex, then add chloroform in the ratio 1:0,25 (methanol:chloroform) and vortex
- centrifuge 1 minute for 14 000 x g at RT
- result is three layers: a large aqueous layer on the top, a circular flake of protein in the interphase and smaller chloroform layer at the bottom
- remove top aqueous layer carefully, try not to disturb the protein flake
- add methanol again in the ratio of 1:1 for the starting sample and vortex
- centrifuge 5 minutes at 20 000 x g which will stick white pellet to the wall of the tube
- remove as much methanol as possible, be careful not to destroy the white pellet

- dry pellet on the bench until all the liquid vaporizes
- resuspend the pellet in the SDS buffer (preheated to 80 °C) and boil for 5 minutes

4.3.10 Immunoprecipitation of proteins

Immunoprecipitation (IP) is one of the most widely used method for isolation of protein and other molecules. IP uses a specific antibody which is coupled with a solid support such as magnetic beads or agarose resin. For the purpose of this theses, magnetic beads were used. The principle of IP is in attaching antibody to magnetic bead and this antibody binds to the tag which is encoded in the protein sequence.

Addition of dithiobis(succinimidyl propionate) (DSP) to the protein sample before incubation with magnetic beads cross-links proteins in the sample so another possible interaction partners would be pulled down altogether with the protein of interest. DSP contains an amine-reactive N-hydroxysuccinimide (NHS) ester at each end of an 8-atom spacer arm (6 carbon atoms plus 2 sulfur atoms). NHS esters react with primary amines at pH 7-9 to form stable amide bonds, along with release of the N-hydroxy-succinimide leaving group. Proteins, including antibodies, generally have several primary amines in the side chain of lysine (K) residues and the N-terminus of each polypeptide that are available as targets for NHS-ester crosslinking reagents.

Dynabeads coupling:

- use Dynabeads™ Protein A Immunoprecipitation Kit
- standard procedure is 1mg of dynabeads to 10 μg of antibody, concentration can be decreased not the other way around
- dynabeads with coupled antibody can be stored at 4 °C up to three months
- we coupled dynabeads with ExBio Original anti-HAHA mouse antibody (working dilution 1:100 000)

Protocol for immunoprecipitation:

- starting volume 250-500 ml of trichomonas culture (of each wild type and transfectants)
- measure the protein content, estimate the amount of culture according to the amount of proteins
- spin the estimated volume of culture and split into two samples, one won't be crosslinked with DSP, so it serves as native sample and the other is treated with DSP
- put the pellet marked as native to the side on ice, proceed with DSP sample
- weigh DSP to be in the final concentration 20mM, dissolve in dimethylsulfoxid (DMSO), vortex
- add DSP in DMSO to the sample and resuspend in PBS
- incubate for 30 minutes at RT
- stop the reaction with TRIS (final concentration 50 mM)
- let sit for 5-10 minutes at RT
- spin at 1250 x g for 10 minutes at 4 °C
- wash with PBS (gently shake, do not use pipette)
- spin at 1250 x g for 10 minutes at 4 °C
- following steps are the same as for DSP and native sample
- add 2X IP buffer:distilled H2O (1:1) and Triton X-100[3] (final concentration 1%), 1 ml of this mixture per 10 mg of protein, resuspend thoroughly
- incubate for 30-45 minutes at 4 °C on a rotator (15 RPM)
- spin at 20 000 x g for 20 minutes at 4 °C
- take supernatant and add dynabeads, invert tube several times
- incubate for 90 minutes at RT on rotator (15 RPM)
- after incubation wash beads two times with IP wash buffer and two times just with IP buffer, aspire the final wash buffer well
- dry dynabeads with coupled antibody linked to protein with HA tag can be processed as a sample for mass spectrometry analysis (protein digestion) or the protein can be eluted in two steps and used for SDS-PAGE analysis

Protein digestion

[3] Triton X-100 will leave proteins in their native conformation, minimizing denaturation of antibody binding sites while at the same time releasing adequate amounts of protein from the sample for subsequent analysis.

(this protocol is derived from the protocol of Karel Harant and Pavel Talacko from Laboratory of Mass Spectrometry, Biocev, Charles University, Faculty of science, where proteomic and mass spectrometric analysis was performed)

- resuspend beads in 100mM tetraethylammonium bromide (TEAB) containing 1 % sodium deoxycholate (SDC)
- reduce cysteines with 5mM final concentration of tris(2-carboxyethyl)phosphine (TCEP) and block with 10mM final concentration of methyl methanethiosulfonate (MMTS)
- cleave samples on beads with 1 µg of trypsin at 37 °C overnight
- centrifuge samples, collect supernatant and acidify supernatant with trifluoroacetic acid (TFA) 1% final concentration
- remove SDC by extraction on ethylacetate (Masuda et al., 2008)
- desalt peptides according to Rappsilbe et al. (2007)

2-step elution:

- add SDS buffer to dynabeads with antibody and protein, mix
- incubate at 65 °C for 10 minutes
- put on the magnet and collect supernatant (keep the dynabeads)
- incubate the supernatant at 95 °C for 5 minutes
- to the dynabeads add SDS buffer and incubate at 95 °C for 5 minutes
- put on the magnet and collect supernatant
- samples can be loaded on the acrylamide gel and analyzed

4.3.11 Quantitative mass spectometry

Samples were analyzed with nano-scale liquid chromatographic tandem mass spectrometry (nLC-MS) according to Herbert et al. (2014). Nano Reversed phase column (EASY-Spray column, 50 cm x 75 µm ID, PepMap C18, 2 µm particles, 100 Å pore size) was used. All data were processed with the MaxQuant software (version 1.6.3.4) (Cox et al., 2014). Quantifications were performed with the label-free algorithm. Data analysis was performed using Perseus 1.6.2.3 software.

4.3.12. Bioinformatic analyses

Initial characteristics of ERMES components were obtained using following bioinformatics tools.

a) **TMHMM Server v. 2.0** (http://www.cbs.dtu.dk/services/TMHMM/)
   - prediction of transmembrane helices in proteins

b) **PSORTII** (https://psort.hgc.jp/form2.html)
   - prediction of protein localization

c) **TargetP 1.1 Server** (http://www.cbs.dtu.dk/services/TargetP/)
   - predicts the subcellular location of eukaryotic proteins

d) **HHpred** (https://toolkit.tuebingen.mpg.de/#/)
   - homology detection and structure prediction

e) **NCBI blast** (https://blast.ncbi.nlm.nih.gov/Blast.cgi)
   - finds regions of similarity between biological sequences

f) **Perseus** (https://maxquant.net/perseus/)
   - protein quantification and analysis of protein interactions

g) **Cytoscape** (https://cytoscape.org/)
   - platform for visualizing complex networks

h) **Geneious** (https://www.geneious.com/)
   - software for DNA data analysis

i) **SWISS MODEL** (https://swissmodel.expasy.org/)
   - fully automated protein structure homology-modelling server

j) **TeeCofee** (http://tcoffee.crg.cat)
   - multiple sequence alignment server

Genomic sequences and gene annotation were obtained from database TrichDB (Aurrecoechea, 2009).

5. RESULTS

5.1. Expression and localization of ERMES components

Initially, we used variety of bioinformatic tools to investigate subunits of the ERMES complex in *T. vaginalis* that are highly divergent proteins. This bioinformatic analysis predicted the localization of ERMES components, presence of transmembrane domains and similarity to other orthologs. Then we attempted to confirm predicted cellular localization using super-resolution microscopy.

5.1.1 Bioinformatic analysis of *T. vaginalis* ERMES components

Mmm1

Putative *mmm1* is a single copy gene (accession number TVAG_214860) that encodes protein of 26,3 kDa, 239 amino acid residues and isoelectric point (pI) 8,09. HMM-HMM comparison of protein sequence using https://toolkit.tuebingen.mpg.de/#/tools/hhpred website found similarity to Mmm1 proteins of *T. foetus* (55,4 %), *S. cerevisiae* (31,4%), *N. Crassa* (23,2 %) and *A. castellani* (23,5 %). Alignment of these proteins using Multiple Sequence Comparison by Log-Expectation (MUSCLE) algorithm showed that Mmm1 is considerably shorter than known orthologs (Fig. 14). However, it possesses the cytoplasm-exposed SMP domain which is characteristic for membrane associated ERMES proteins.

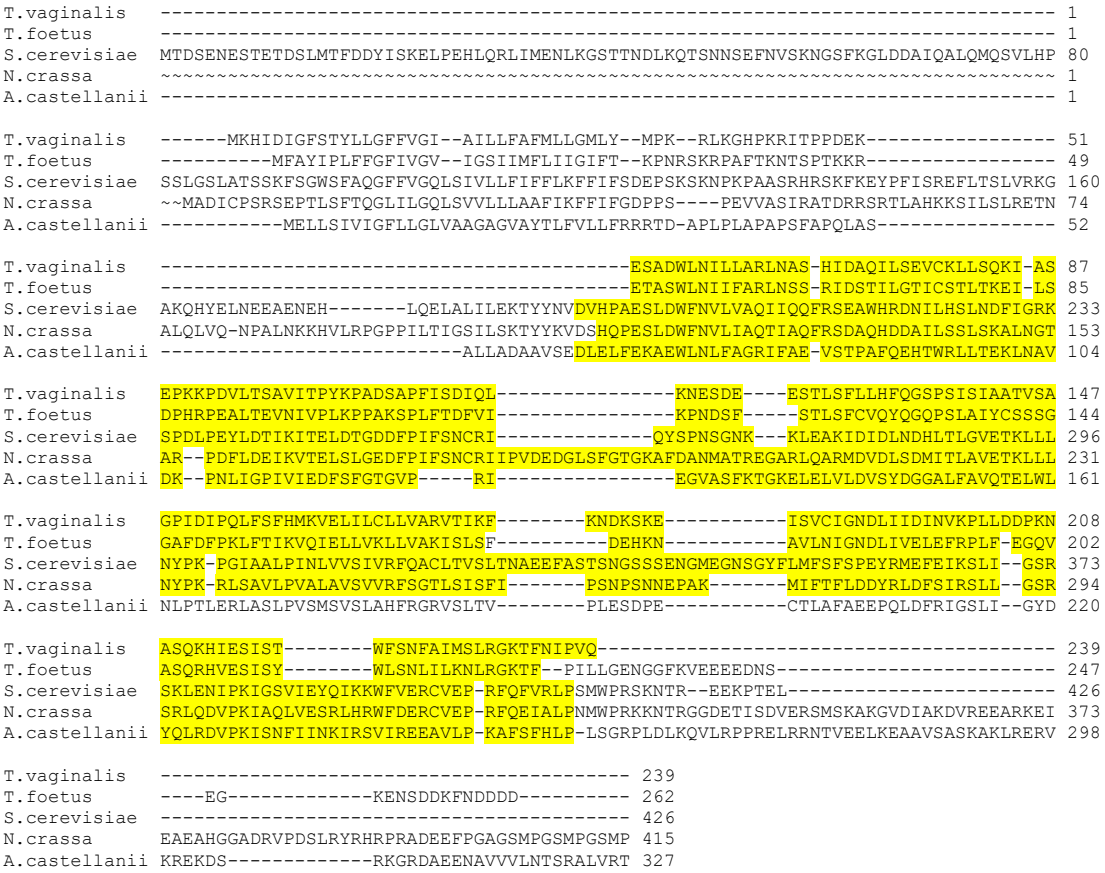

Figure 14. Protein sequence alignment of *T. vaginalis* Mmm1 and selected orthologs. Search for conserved domains using InterProScan server revealed presence of SMP domains (in yellow) at 50-239 AA position in *T. vaginalis* Mmm1. *T. foetus*, *Tritrichomonas foetus* (accession number TRFO_40493); *S. cerevisiae*, *Saccharomyces cerevisiae* (uniprot accession number P41800-1); *N. crassa*, *Nerospora crassa* (uniprot accession number Q9P353-1); *A. castellanii*, *Acantamoeba castellanii* (uniprot accession number A0A0H3YBY9-1).

Prediction of transmembrane domains using TMHMM Server v. 2.0 showed a single transmembrane domain close to the N-terminus (Fig. 15).

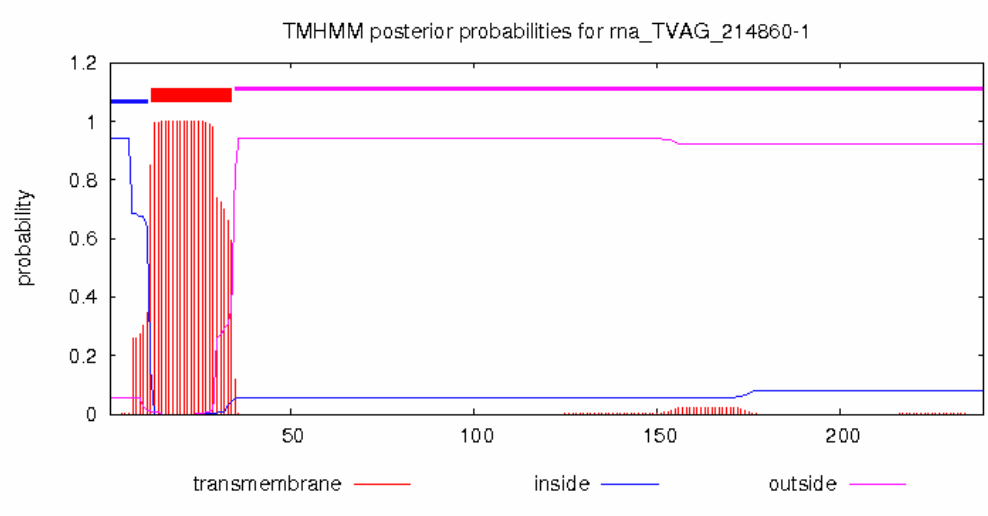

Figure 15. TMHMM prediction of transmembrane domains for Mmm1. A single transmembrane domain is strongly supported between amino acid residues 12-34.

Prediction of Mmm1 cellular localization using PSORT II predicted Mmm1 to reside in ER with 44,4 % probability. Signal peptide prediction using TargetP 1.1 and SignalP-5.0 did not find targeting sequences.

Mmm2a and Mmm2b

Homology searches for Mmm2 in *T. vaginalis* genome revealed presence of two paralogs with high protein sequence similarity (95,8 %). Putative *mmm2a* gene (accession number TVAG_217400) encodes protein of 21,6 kDa, 190 amino acid residues with pI 9,82. Putative *mmm2b* gene (accession number TVAG_375920) encodes protein of 21,6 kDa, 190 amino acid residues and with pI 9,91.

HMM-HMM comparison revealed the highest similarity of Mmm2b to Mmm2 proteins of *T. foetus* (67,9 %), whereas only 18,7 % when compared with Mmm2 of *S. cerevisiae* (Fig. 16).

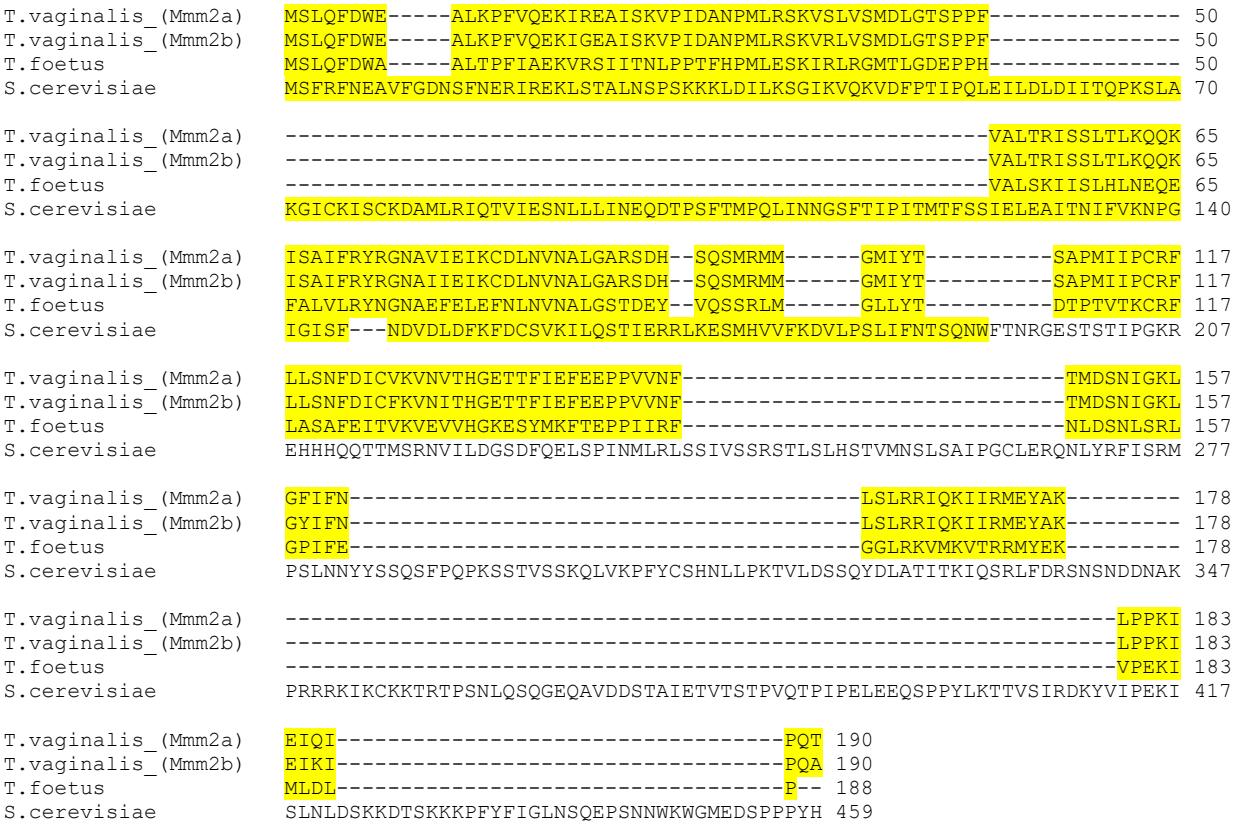

Figure 16. Protein sequence alignment of *T. vaginalis* Mmm2 and selected orthologs. Search for conserved domains using InterProScan revealed SMP domains (in yellow) at 1-190 AA position in *T. vaginalis* Mmm2. *T. foetus*, *Tritrichomonas foetus* (accession number TRFO_30611); *S. cerevisiae*, *Saccharomyces cerevisiae* (uniprot accession number P53083-1).

Prediction of transmembrane domains using TMHMM Server v. 2.0 showed transmembrane domain with significant support in neither Mmm2a (Fig. 17) nor Mmm2b (Fig. 18).

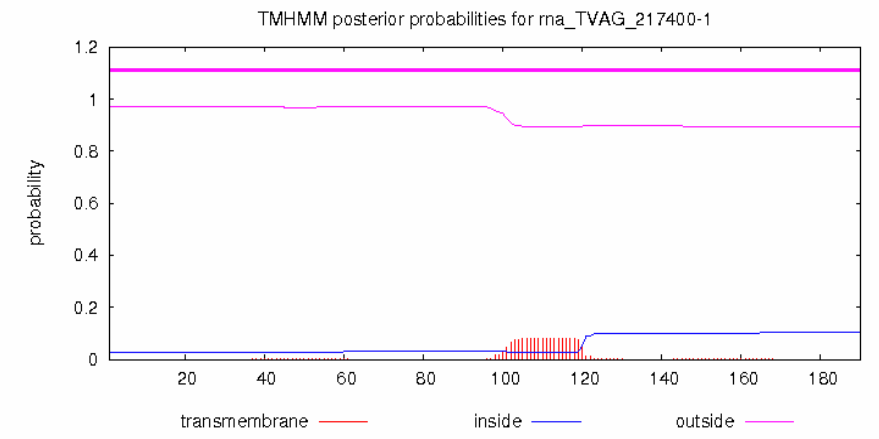

Figure 17. TMHMM prediction for transmembrane domains of Mmm2a.

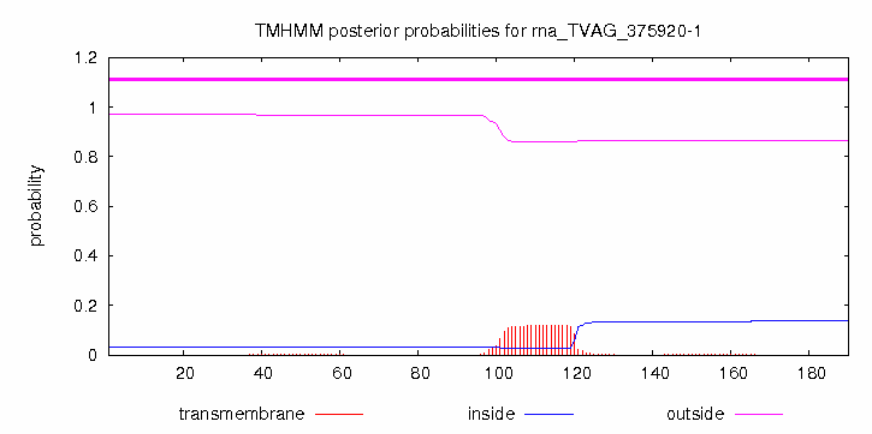

Figure 18. TMHMM prediction for transmembrane domains of Mmm2b.

Prediction of cell localization using PSORT II revealed the highest probability for cytosolic localization with 47.8 % for Mmm2a and 69,6 % for Mmm2b. Probability for expected mitochondrial localization was scored only to 8,7 % for Mmm2a. PSORTII did not find any probability for Mmm2b to be the mitochondrion bound protein.

Mdm12

Putative *mdm12* is a single copy gene (accession number TVAG_063000) that encodes protein of 23,6 kDa, 207 amino acid residues with pI 4,65. HMM-HMM showed moderate similarity of *T. vaginalis* Mdm12 to *T. foetus* ortholog (57,1 %) and lower similarity to *S. cerevisiae* (32,2 %) and *D. purpureum* (37,4 %).

```
T.vaginalis   -------------------------------------------MSLRINWDALQSYVVQERTIEYITQMFLNALKDSPE 36
T.foetus      MILLDQNFIQNITKYQLKYLLMKCELKTLIKDLIDIFKRSLFSKMNIEVNMDALQSYVIEDKTSQFITNAVMELLNKSDK 80
S.cerevisiae  -------------------------------------------MSFDINWSTLESDNRLNDLIRKHLNSYLQN-TQLPS 35
D.purpureum   -------------------------------------------MSLKIYWDRITEKHSIK--LMNHLNQQLSGLTKTYE 34

T.vaginalis   FSSTFMVNTLSFGTIPPTIDIISMKD------------------------------IDVKLQWHLKTHIY--------E 77
T.foetus      FSATFDIENLKFGTKQPTVQLISMKD------------------------------VDVTLQWHLNTHEFIIPSFKQSN 129
S.cerevisiae  YVSNLRVLDFDLGKVGPAITLKEITDPLDEFYDSIREEADQETEENNDNKEDSEHICPDRTIANHEGPKD---------D 106
D.purpureum   NIGELKLSNLSLGSKPPTFEIIQISD------------------------------PDALI---LGTKS---------- 70

T.vaginalis   LPQLQQIPFNAPFQATVSINWESNGSFAFSACLSYDKIAPGCIKFPFNASISNLSISGKLCILYLGDAIIAFF------- 150
T.foetus      MPFLKSFEFQAPFQAVISVYCKSDCSISISTTLSFDGISPGCIKFPIHATISHIEFTGQITVQYLGDSIVLFF------- 202
S.cerevisiae  FEAPVVMPSPNDIQFLLEVEYKGDLLVTIGADLVLNYPVEKFMTLPVKLSISDIGLHSLCIVACLSKQLFLSFLCDVSDP 186
D.purpureum   ---------PNGIELRAKIGYEGDAFIIVQTEFKVNLPTPNFITFPVTVKVSNPKFSGIASVIYDTDKVCFCFV-----P 136

T.vaginalis   -------EKDP----------------DFNFQLELSLGAEEK-----VFDQHQVRDLICEILRGWTSDNIVHPNSLKFPF 202
T.foetus      -------EVPP----------------DFHFDLDLVLGAEEK-----FFDQYQVRGFISEVLNDWMTKNLVHPNAIKLPI 254
S.cerevisiae  ALDDNQTVLDPKGPILAATKPLERISIVRSMKIETEIGEQYQGQGSVLRSVGELEQFLFTIFKDFLRKELAWPSWINLDF 266
D.purpureum   PADNSEGDYTP----------------LKDFKFETQLGDSDQ---HVLADLDKLENFIVGEIKSLLKKYLVYPNKLTVLL 197

T.vaginalis   NQPTQ- 207
T.foetus      SED--- 257
S.cerevisiae  NDGDE  271
D.purpureum   SDFN-- 201
```

Figure 19. Protein sequence alignment of *T.vaginalis* Mdm12 and selected orthologs. Search for conserved domains using InterProScan revealed SMP domains (in yellow) at 1-203 AA position in *T. vaginalis* Mdm12. *T. foetus*, *Tritrichomonas foetus* (accession number TRFO_36785); *S. cerevisiae*, *Saccharomyces cerevisiae* (uniprot accession number Q92328-1); D. purpureum, *Dictyostelium purpureum* (uniprot accession number F0ZU49-1).

Prediction of the transmembrane domains using TMHMM Server v. 2.0 showed no transmembrane domains to be present (Fig. 20). Prediction of Mdm12 localization by PSORT II revealed the highest probability for the cytosolic localization (56,5 %).

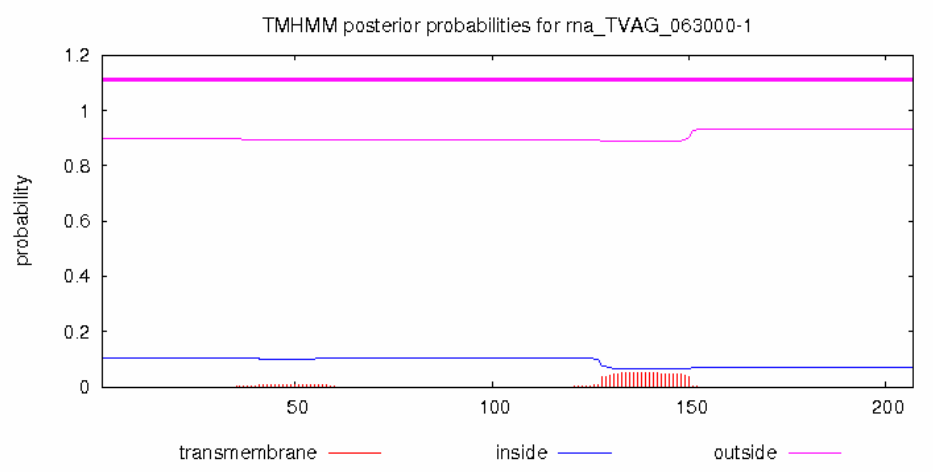

Figure 20. TMHMM prediction for transmembrane domains of Mdm12.

5.1.2 Localization of ERMES components using super-resolution microscopy

In the next step we subcloned genes for Mmm1, Mmm2a, Mmm2b and Mdm12 to TagVag2 plasmid that allows expression of corresponding proteins with HA tag at the C terminus under control of the α-subunit of SCS promoter. T1 strain of *T. vaginalis* was transfected using electroporation and transfectants were selected with geneticin. Transfectants were tested for expression of recombinant proteins by SDS-PAGE and Western blotting (Fig. 21). Lineages that expressed proteins with expected molecular weight were used for further experiments. The molecular weights observed on western blots were slightly higher for Mmm1 and Mmm2 proteins than molecular weights calculated based on protein sequences. This might be caused by post-translational modifications such as glycosylation.

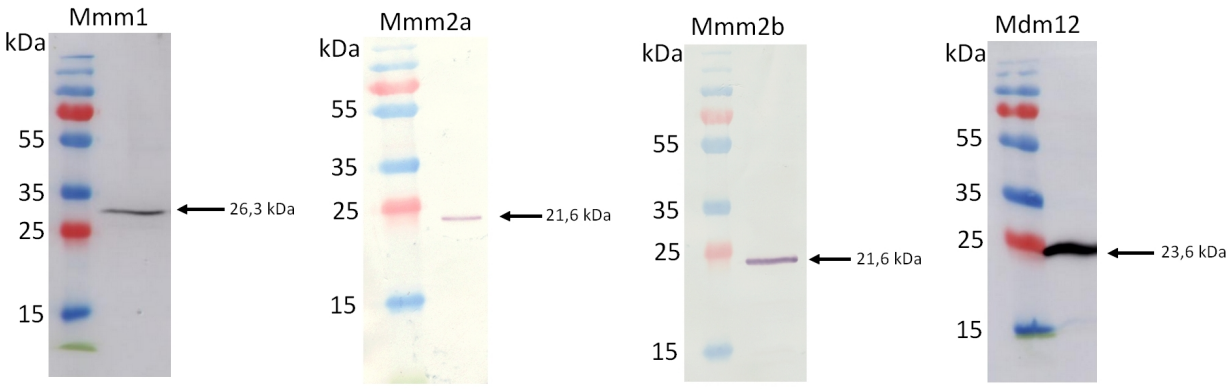

Figure 21. SDS-PAGE and Western blot analysis of expressed proteins in *T. vaginalis*. Arrows point to specific bands corresponding to HA-tagged recombinant protein. All components were detected by antibody (Ab) against HA tag.

Mmm1 was expected to localize to ER. As we have no suitable Ab against any ER marker protein, Mmm1 was co-expressed in lineage that was previously transfected with plasmid for expression of V5-tagged soluble protein disulfide-isomerase (SPDI) (Rada et al., 2011). Localization of Mmm2 and Mdm12 was studied in single transformants and co-localized with malic enzyme using specific malic enzyme Ab (Drmota et al., 1996). The localization of ERMES components was investigated using structured illumination microscopy (SIM).

Mmm1-HA was observed as a ring around the nucleus and in numerous small spots scattered within the cytosol (Fig. 22). The similar structures were labeled with antibodies against ER marker protein SPDI-V5 that mostly co-localized with Mmm1-HA.

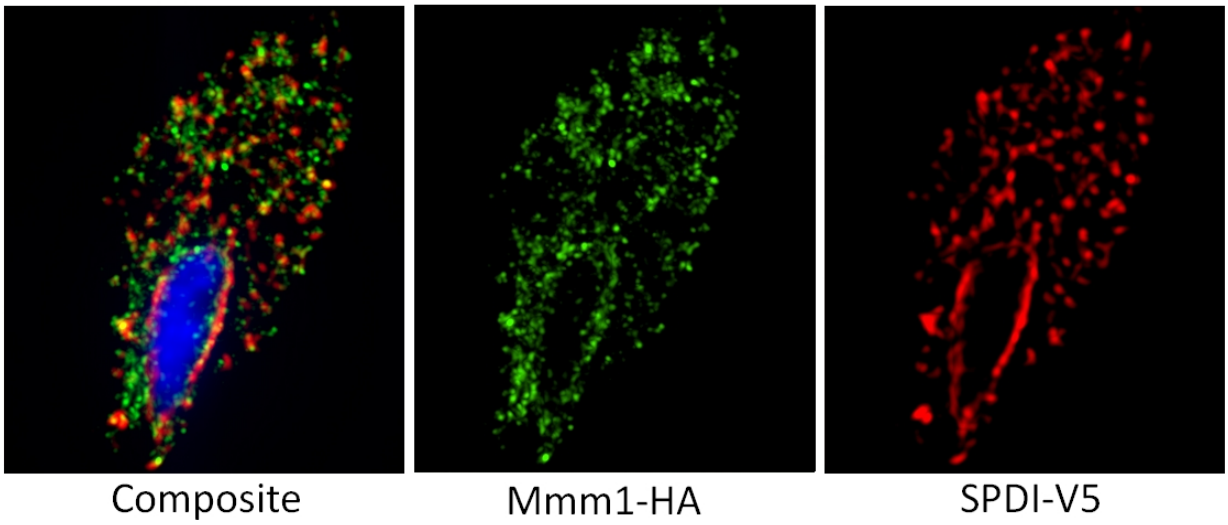

Figure 22: Cellular localization of Mmm1 in *T. vaginalis* using SIM.
Mmm1 was expressed with a C-terminal HA tag and visualized with a mouse monoclonal anti-HA Ab (green). ER marker SPDI was expressed in trichomonads with a C-terminal V5 tag and detected with a rabbit monoclonal anti-V5 Ab (red). The nucleus was stained with DAPI (blue).

Mmm2a-HA was detected in small spots within the cell. These spots were apparently smaller than vesicles corresponding to hydrogenosomes that were visualized by malic enzyme Ab. Mmm2a-HA spots were in some cases observed in close proximity of hydrogenosomes and partially co-localized (Fig. 23).

Similar pattern was observed in cells expressing Mmm2b-HA (Fig. 24). Mmm2b-HA was located in small spots that partially co-localized with hydrogenosomes.

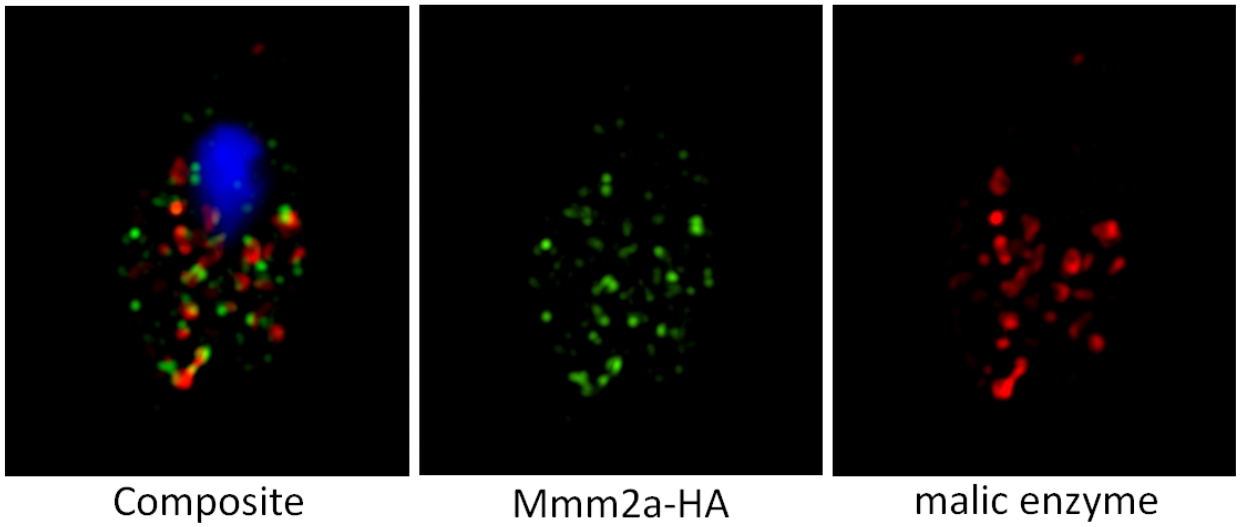

Figure 23. Localization of Mmm2a in *T. vaginalis* using SIM.

Mmm2a was expressed with a C-terminal HA tag and visualized with a mouse monoclonal anti-HA Ab (green). The hydrogenosomal marker malic enzyme was detected with a polyclonal rabbit anti-malic enzyme Ab (red). The nucleus was stained with DAPI (blue).

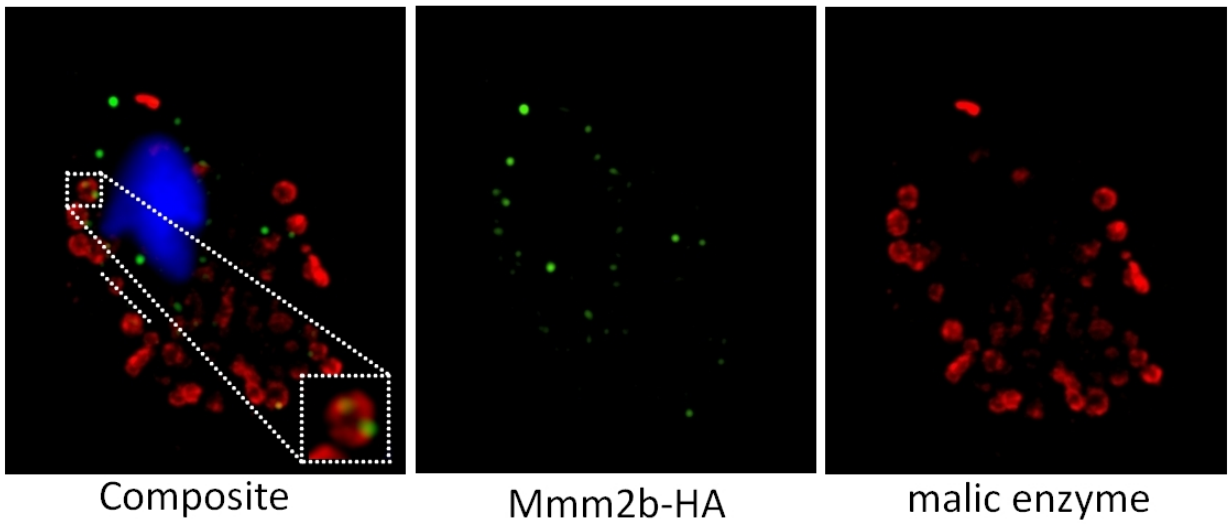

Figure 24. Localization of Mmm2b in *T. vaginalis* using SIM.

Mmm2b was expressed with a C-terminal HA tag and visualized with a mouse monoclonal anti-HA Ab (green). The hydrogenosomal marker malic enzyme was detected with a polyclonal rabbit anti-malic enzyme Ab (red). The nucleus was stained with DAPI (blue).

To further investigate whether Mmm2 is localized on the hydrogenosomal membrane, Mmm2b with V5 tag was co-expressed in *T. vaginalis* together with HA-tagged Tom40 subunit of translocase of outer hydrogenosomal membrane (TOM). Tom40 was visualized as rings, half rings or spots. Both Mmm2a and Mmm2b were observed as spots with distribution similar to Tom40. In few ring-like structures, both Tom40 - Mmm2a and Tom40 - Mmm2b signals were observed (Fig. 25 and 26).

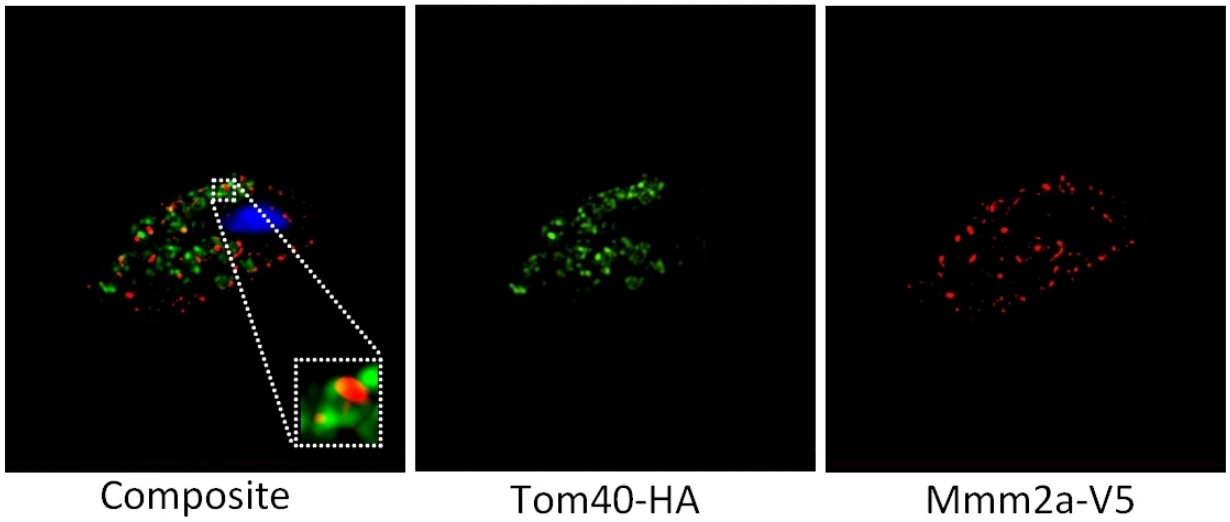

Figure 25. Localization of Mmm2a and Tom40 in *T. vaginalis* using SIM microscopy.
Mmm2a was expressed with a C-terminal V5 tag and visualized with a rabbit monoclonal anti-V5 Ab (red). Tom40 was expressed in trichomonads with C-terminal HA tag and detected with a mouse monoclonal anti-HA Ab (green). The nucleus was stained with DAPI (blue).

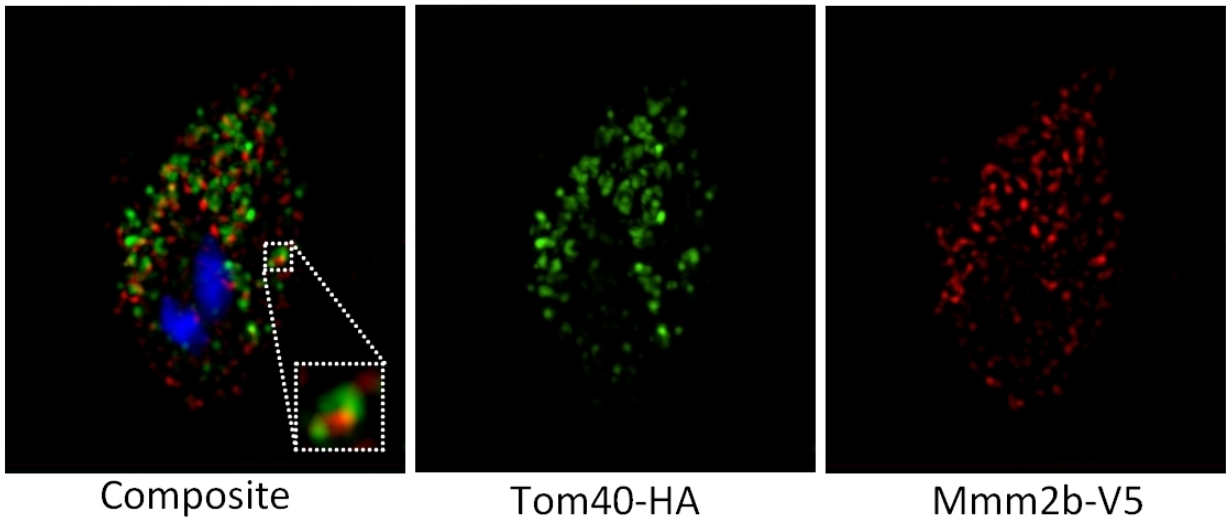

Figure 26. Localization of Mmm2b and Tom40 in *T. vaginalis* using SIM.
Mmm2b was expressed with a C-terminal V5 tag and visualized with a rabbit monoclonal anti-V5 Ab (red). Tom40 was expressed in trichomonads with C-terminal HA tag and detected with a mouse monoclonal anti-HA Ab (green). The nucleus was stained with DAPI (blue).

Mdm12 appeared within the cell in numerous spots partially co-localizing with hydrogenosomes (Fig. 27) as Mmm2a-HA and Mmm2b-HA.

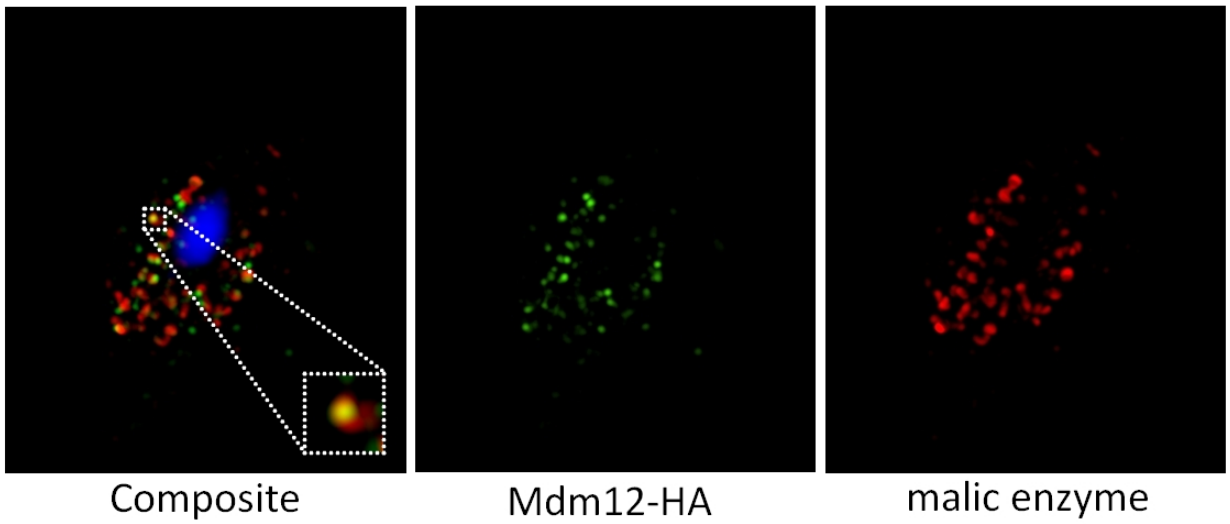

Figure 27. Localization of Mdm12 protein in *T. vaginalis* using SIM.
Mdm12 was expressed with a C-terminal HA tag and visualized with a mouse monoclonal anti-HA Ab (green). The hydrogenosomal marker malic enzyme was detected with a polyclonal rabbit anti-malic enzyme Ab (red). The nucleus was stained with DAPI (blue).

5.1.3 Super-resolution microscopy of Mmm1 and Mmm2 in double transfectants

To investigate whether Mmm1 and Mmm2 interact with each other, both proteins were co-expressed in *T. vaginalis* with HA and V5 tag at the C terminus, respectively. We observed both Mmm1-HA and Mmm2b-V5 as small spots within the cell that mostly did not co-localize. Nevertheless, few signals of Mmm1-HA and Mmm2b-V5 co-localized or they were in close proximity (Fig. 28).

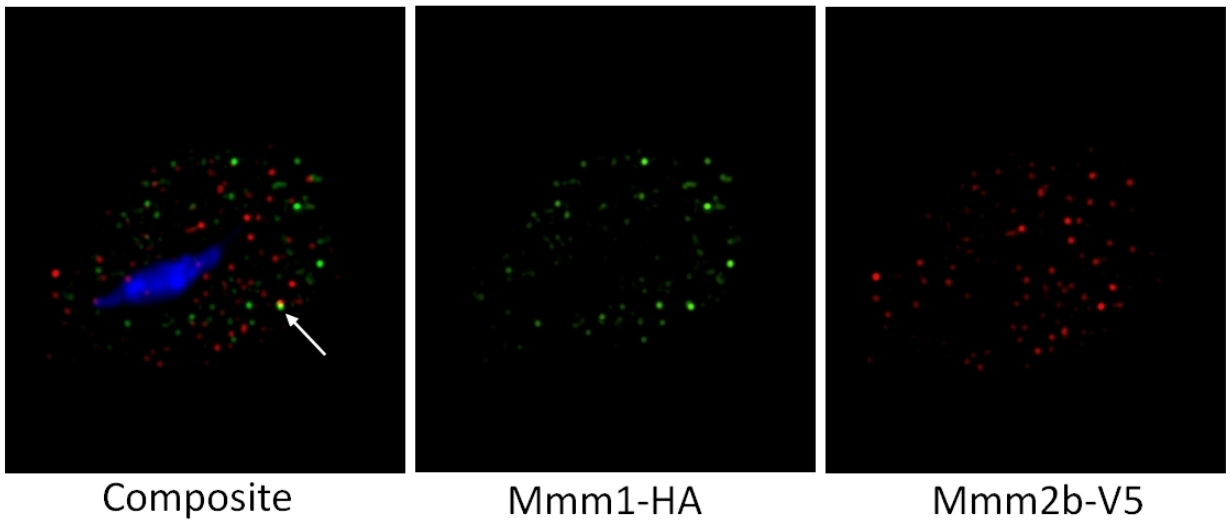

Figure 28. Localization of Mmm1 and Mmm2b in *T. vaginalis* using SIM.
Mmm1 was expressed with a C-terminal HA tag, here visualized with a mouse monoclonal anti-HA Ab (green). Mmm2b was expressed in trichomonads with a C-terminal V5 tag and detected with a rabbit monoclonal anti-V5 Ab (red). The nucleus was stained with DAPI (blue). Arrowhead indicates co-localization of Mmm1 and Mmm2.

5.2 Identification of Mmm2 in subcellular fractions

The results from immunofluorescence microscopy were supported by Mmm2 localization in subcellular fractions. Cells that expressed Mmm2a and Mmm2b were homogenized by sonication and cell fractions were separated using Percoll gradient. Fractions were analysed by SDS-PAGE and Western blotting (Fig. 29). Western blot analysis revealed the strongest signal for Mmm2a in the hydrogenosomal fraction. The protein forms a double band of molecular weight about 21 and 22 kDa. However, weaker signal was also detected in LDV that contains

lysosomes and vesicles of ER (Štáfková et al., 2018). Similarly, Mmm2b showed the strongest signal in hydrogenosomal fraction, whereas weaker band was observed in the LDV and in the cytosol.

These results indicate that both paralogs of Mmm2 are associated with the hydrogenosomes, however they might be present also in other cellular compartments.

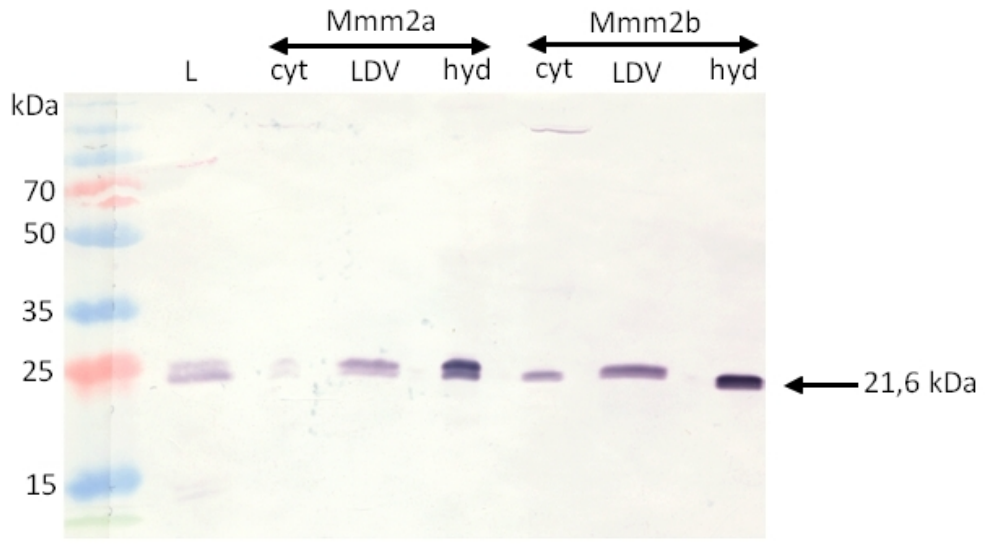

Figure 29. Detection of Mmm2 in *T. vaginalis* subcellular fractions using Western blot analysis. *T. vaginalis* cells expressing Mmm2a and Mmm2b were separated using Percoll gradient centrifugation. **L** – cell lysate, **cyt** – cytosolic fraction, **LDV** – low density vesicles, **hyd** – hydrogenosomal fraction. Mmm2a and Mmm2b were detected by antibody against HA tag.

5.3 Topology of Mmm2

To investigate topology of Mmm2a and Mmm2b in hydrogenosomes, we performed protease protection assay. Hydrogenosomes isolated from *T. vaginalis* cells that expressed Mmm2a and Mmm2b were incubated with or without proteinase K. Proteinase K treatment resulted in disappearance of Mmm2 proteins and C-tail anchored protein CTA10 which was used as a control outer membrane protein (Fig. 30). The treatment with proteinase K did not affect signal for β subunit of SCS, which is localized in the hydrogenosomal matrix and it is protected by hydrogenosomal membranes. These results demonstrated that both paralogs of Mmm2 are not

protected by the hydrogenosomal membranes and they are attached to the outer hydrogenosomal membrane facing to the cytosol.

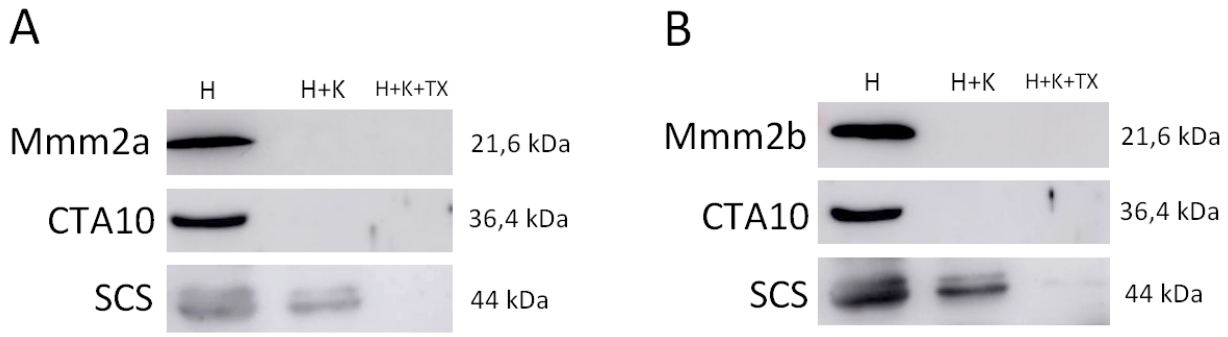

Figure 30. Protein protection assay of Mmm2a (A) and Mmm2b (B). Hydrogenosomes were isolated from the strain expressing Mmm2a-HA or Mmm2b-HA (H) and treated with proteinase K (H+K) or proteinase K together with detergent Triton X-100 (H+K+TX). Mmm2a and Mmm2b were detected by antibody against HA tag, β subunit of SCS was detected by anti β subunit of SCS polyclonal rabbit antibody, CTA10 was detected by anti CTA10 rabbit polyclonal antibody**.**

5.4. Immunoprecipitation of ERMES components

To investigate interactions between ERMES components, we immunoprecipitated Mmm1, Mmm2b and Mdm12 from cell lines expressing HA-tagged versions of these proteins.

5.4.1 Immunoprecipitation of Mmm1

First, we performed immunoprecipitation of Mmm1-HA protein under native conditions and with stabilization of protein interactions using DSP crosslinker (see chapter 4.3.10). SDS-PAGE and Western blot analysis revealed higher yield of immunoprecipitated protein in cells that were treated with DSP (Fig. 31). For further experiments with Mmm2b and Mdm12 we decided to use only DSP treated cells.

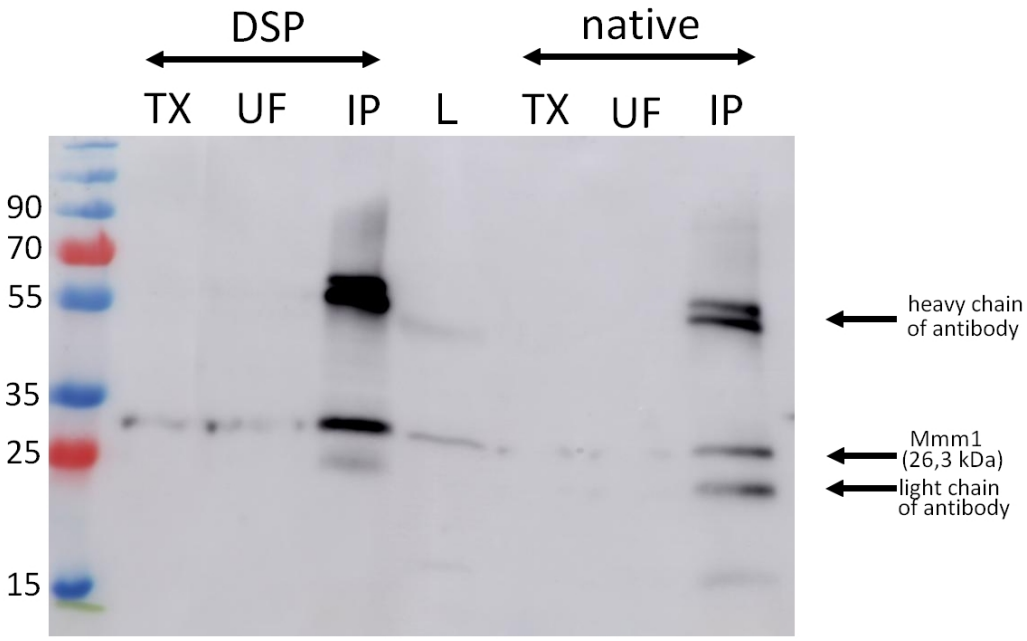

Figure 31. Western blot analysis of Mmm1 co-immunoprecipitated proteins.
IP was performed using DSP treated cells or under native conditions. TX – sample of cells that were treated with Triton X–100 (supernatant with present protein), UF – unbound fraction (sample of protein that did not bind to dynabeads), IP – immunoprecipitated proteins, L – lysate of cells expressing Mmm1-HA.

When we established the final IP protocol, we performed IP in triplicates with DSP treated Mmm1-HA cell line and wild type cells. Proteins that were pulled down with Dynabeads were submitted for label-free quantitative (LFQ) mass spectrometry. The Mmm1 sample that was analyzed by mass spectrometry contained 1739 proteins (Table 3-A in supplementary data at CD disk). Next we analyzed data with Perseus (version 1.6.6.0) software to test statistical support for expected protein interactions. To analyze the LFQ MS data, first we replaced missing LFQ intensities values for proteins that were identified only for Mmm1 cell line or in wild type. Missing values (0) were replaced by random low numbers calculated with "Imputation" tool of Perseus. To analyze the correlation between samples we performed Multi-scatter plot analysis, which plots all samples against each other (Fig. 32). The Pearson correlation coefficient (which is a measure of the linear correlation between two variables X and Y, where 1 is total correlation and 0 is no linear correlation) suggests that the consistency of the obtained data was not optimal (Pearson coefficient range 0,579-0,975).

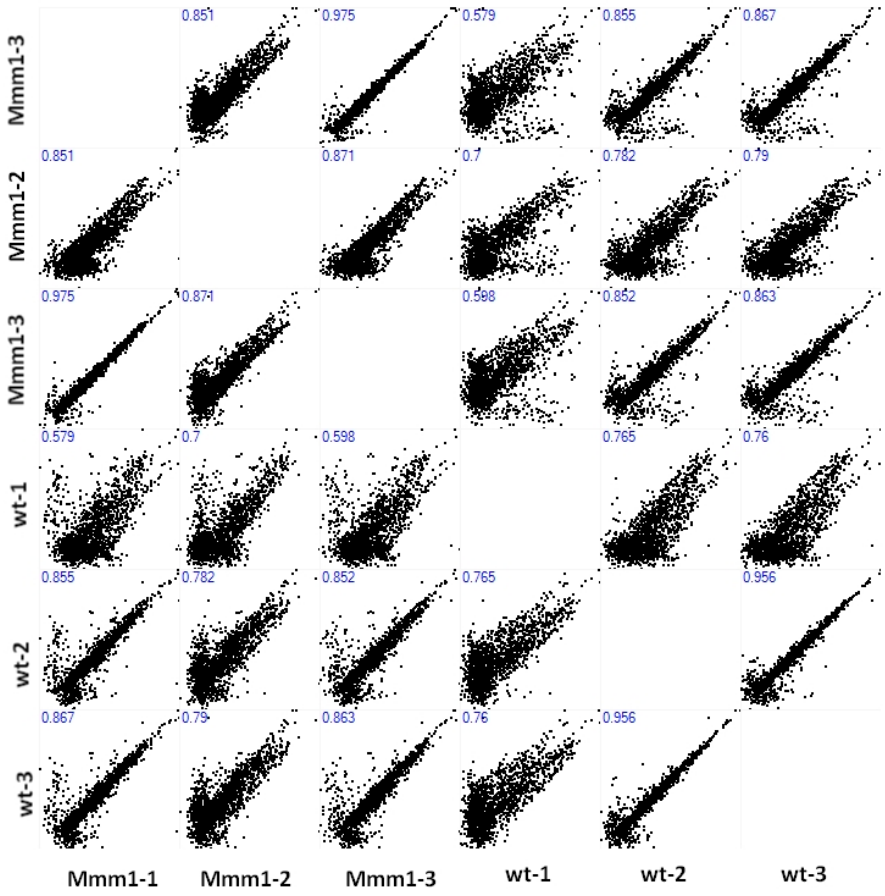

Figure 32. Multi-scatter plot analysis of data obtained for triplicates of Mmm1 (Mmm1-1, Mmm1-2, Mmm1-3) against data for triplicate of controls (wt-1, wt-2, wt-3). Numbers in the left upper corner represent the value of Pearson coefficient.

Next we performed Volcano plot analysis (Fig. 33). The Volcano plot (-log10 p-value plotted against the corresponding t-test difference) is the unified function of two sample t-test and scatter plot. The cut-off curve, assigning significant interactors, is based on the false discovery rate (FDR) and the artificial factor s0. s0 controls the relative importance of the t-test p-value and difference between means. At s0=0 only p-value matters, while at nonzero s0 the difference of means contributes.

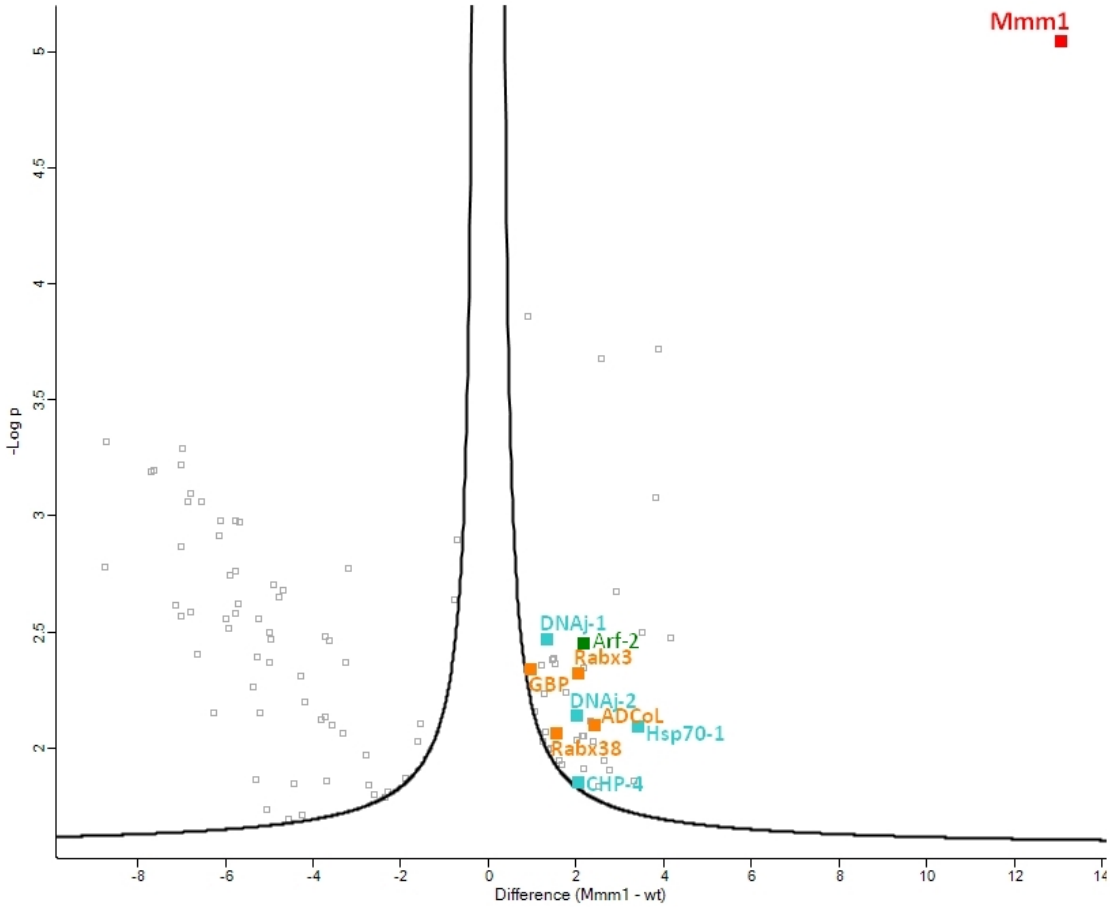

Figure 33. Volcano plot displayed proteins that immunoprecipitated with Mmm1 with significant statistical support. The vertical axis corresponds to the mean value of -log p-value and the horizontal axis displays corresponding t-test difference. Blue squares represent proteins that were found to interact with Mmm2b and Mdm12 in following experiments (Fig. 42). Green square represents protein that co-immunoprecipitated with Mmm2b. Orange squares depict proteins that were found to interact with Mdm12. Red square represents Mmm1. S0=0,1; FDR=0,05

Volcano plot analysis revealed altogether 42 significantly enriched proteins (Table 4, Table 4 in supplementary data at CD disc.), however neither Mmm2 nor Mdm12 were present in this dataset as expected.

To get more information on co-immunoprecipitated proteins, we analyzed their protein sequences by various bioinformatic tools that predict the presence of conserved domains (Interproscan), transmembrane domains (TmHMM), cell localization (PSORTII) and signal peptides (TargetP). We used NCBI BLAST and HHpred for protein homology searches (Tab. 4).

Table 4. *In silico* analysis of Mmm1 co-immunoprecipitated proteins

Label	Protein name	Accession number	Interproscan (domain)	TmHMM	PSORTII	TargetP	NCBI	HHpred
Mmm1	Mmm1	TVAG_214860	SMP	1	ER	no	no hint	Mmm1
CHP-1	conserved hypothetical protein	TVAG_436670	no hint	0	cytoplasmic	no	no hint	eIF4 gamma subunit
CHP-2	conserved hypothetical protein	TVAG_133500	family PTHR33023:SF506	0	nuclear	no	surface immunogen P270-related protein	Ig-like domain
CHP-3	conserved hypothetical protein	TVAG_325080	metallo-beta-lactamase	0	cytoplasmic	no	metallo-beta-lactamase superfamily	metallo-beta-lactamase
CHP-4	cysteine protease	TVAG_514800	myeloid leukemia factor	0	nuclear	no	cysteine protease	myeloid leukemia factor
CHP-5	conserved hypothetical protein	TVAG_081570	no hint	0	nuclear	no	no hint	abl interactor 1
CHP-6	conserved hypothetical protein	TVAG_070000	no hint	0	ER	SP	no hint	nodal modulator 3-like
CHP-7	Mmm1a-like	TVAG_194830	no hint	0	cytoplasmic	no	no hint	Mmm1
CHP-8	conserved hypothetical protein	TVAG_431140	2 TM helices	2	ER	no	no hint	no hint
CHP-9	Mmm1c-like	TVAG_302900	1 TM helix	1	extracellular	SP	no hint	Mmm1
Hsp70-1	Hsp70-1	TVAG_291920	Hsp70/DNAk	0	nuclear	no	DnaK	Hsp70
DnaJ-2	DnaJ-2	TVAG_317210	Hsp40/DNAj	0	cytoplasmic	no	DnaJ	DnaJ
DnaJ-1	DnaJ-1	TVAG_305730	Hsp40/DNAj	0	nuclear	no	DnaJ	DnaJ
ADCoL	AMP dependent CoA ligase	TVAG_337850	AMP-dependent synthetase/ligase	0	cytoplasmic	no	AMP-binding protein	long-chain-fatty-acid-CoA ligase
Rabx3	ras related protein	TVAG_008100	small GTP-binding protein	0	cytoplasmic	no	small GTP-binding protein	ras related protein
Rabx38	ras related protein	TVAG_104710	small GTP-binding protein	0	cytoplasmic	no	small GTP-binding protein	ras related protein
GBP	ras related protein	TVAG_190510	small GTP-binding protein	0	cytoplasmic	no	small GTP-binding protein	ras related protein
Arf-1	ADP-ribosylation factor	TVAG_294070	small GTP-binding protein	0	cytoplasmic	M	small GTP-binding protein	ADP-ribosylation factor
Arf-2	ADP-ribosylation factor	TVAG_262220	small GTP-binding protein	0	cytoplasmic	no	ADP-ribosylation factor	ADP-ribosylation factor
actin	actin	TVAG_094140	actin	0	mitochondrial	no	actin family protein	actin
actin2	actin	TVAG_337240	actin	0	cytoplasmic	no	actin	actin
RAB-1	ras related protein	TVAG_310110	small GTP-binding protein	0	mitochondrial	no	small GTP-binding protein	ras related protein
RAB-2	ras related protein	TVAG_430220	small GTP-binding protein	0	cytoplasmic	no	small GTP-binding protein	ras related protein
RAB-3	ras related protein	TVAG_527180	small GTP-binding protein	0	cytoplasmic	no	small GTP-binding protein	ras related protein
Rab11	ras related protein	TVAG_047800	small GTP-binding protein	0	cytoplasmic	SP	Ras-like related protein	ras related protein
Rab15	ras related protein	TVAG_454230	small GTP-binding protein	0	cytoplasmic	no	Ras family protein	ras related protein
Rabx18	ras related protein	TVAG_324930	small GTP-binding protein	0	ER	no	small GTP-binding protein	ras related protein
Rab20	ras related protein	TVAG_498380	small GTP-binding protein	0	cytoplasmic	no	small GTP-binding protein	ras related protein
Rab21-1	ras related protein	TVAG_169920	small GTP-binding protein	0	cytoplasmic	no	small GTP-binding protein	EF-hand calcium binding domain
Rab21-2	ras related protein	TVAG_388780	small GTP-binding protein	0	ER	M	Ras family protein	ras related protein
Rabx30	ras related protein	TVAG_093060	small GTP-binding protein	0	cytoplasmic	no	Ras family protein	ras related protein
Rabh	ras related protein	TVAG_440690	small GTP-binding protein	0	cytoplasmic	no	small GTP-binding protein	ras related protein
Rheb	ras related protein	TVAG_533910	small GTP-binding protein	0	cytoplasmic	no	small GTP-binding protein	ras related protein
Rabi	ras related protein	TVAG_092740	small GTP-binding protein	0	cytoplasmic	no	small GTP-binding protein	ras related protein
Arp2/3	actin related protein 2/3	TVAG_083290	Arp2/3	0	cytoplasmic	no	actin related	Arp2/3

							protein	
PABP-1	polyadenylate-binding protein	TVAG_110950	RNA-binding domain	0	cytoplasmic	no	polyadenylate-binding protein	RNA-binding protein
Pyr	pyrazinamidase/nicotinamidase	TVAG_366320	isochorismatase-like	0	cytoplasmic	no	isochorismatase family protein	pyrazinamidase/nicotinamidase
MIMP	myo inositol monophosphatase	TVAG_308070	inositol monophosphatase	0	cytoplasmic	no	inositol monophosphatase	inositol monophosphatase
MLSP	methylesterase-like serine peptidase	TVAG_008710	alpha/beta hydrolase fold-1	1	extracellular	SP	methylesterase-like serine peptidase	fatty acid ethyl ester synthase/esterase
FGF	fibroblast growth factor	TVAG_099320	NUDIX hydrolase domain	0	nuclear	no	hydrolase, NUDIX family	NUDIX hydrolase
AHPR/C	alkyl hydroperoxide reductase	TVAG_075420	thioredoxin domain	0	cytoplasmic	no	tryparedoxin peroxidase	thioredoxin
Hsp70-3	Hsp70-3	TVAG_300470	Hsp70	0	cytoplasmic	no	cytoplasmic Hsp70	Hsp70

SP-secretory pathway, M-mitochondrion.

Bioinformatical analysis of these proteins suggests that Mmm1 is likely associated with ER membrane facing the cytosol. Proteins with accession number TVAG_431140, TVAG_388780, TVAG_324930 and TVAG_070000 could be associated with ER according to *in silico* prediction. We found number of Rab small GTPases, which are involved in vesicular transport pathways (Novick et al., 1997). We also identified two Arf paralogs, which could be linked to ERMES function (Rabouille, 2014). We aligned protein sequences of these two Arf proteins with Arf1 of *S. cerevisiae* and found similarity 59,1 % for TVAG_262220 and 61,1 % for TVAG_294070.

Surprisingly, HHpred searches using CHP-7 as query revealed homology to Mmm1 of *Zygosaccharomyces rouxii* with e-value $7{,}4^{-22}$ and other Mmm1 proteins of fungi. BLAST search against *T. vaginalis* protein database at TrichDB revealed two proteins with highest e-values, TVAG_139550 (e-value $1e^{-26}$) and Mmm1 (TVAG_214860, E 0,48). HHpred searches also revealed that CHP-9 shares some homology with Mmm1 proteins. We name these homologs Mmm1a-like (CHP-7), Mmm1b-like (TVAG_139550) and Mmm1c-like (CHP-9) proteins. Protein sequence alignment using TeeCofee server (Fig. 34) revealed conserved region shared by Mmm1 and Mmm1-like proteins.

```
TVAG_214860/Mmm1         MKHIDIGFSTYLLGFFVGIAILLFAFMLLGML--YMPKRL------KGHP 42
TVAG_302900/Mmm1c-like   MNIL--------LSFFLGVLFSLPVFVLFLLLLSFLTGKIIKKRRNTLRK 42
TVAG_139550/Mmm1b-like   MEL---------------------------------------------- 3
TVAG_194830/Mmm1a-like   MFG----------------------------------------------T 4

TVAG_214860/Mmm1         KRITPPDEKESADWLNILLARLNASHIDAQILSEVCKLLSQKIASE---- 88
TVAG_302900/Mmm1c-like   EPAFTVGTMCTVSWLNSIVQRVFLIAVTKKSLTFIIKSAIPKITEKTPLT 92
TVAG_139550/Mmm1b-like   ---QSKPVTESTDWLNFSIERFMEIVDSPEGLEKLSNAISNAMAPN---- 46
TVAG_194830/Mmm1a-like   RPIPYKMTKESTDWLNFIIYRVLTHFQTPESIAKINALVNDKVKPA---- 50

TVAG_214860/Mmm1         PKKPDVLTSAVITPYKPADSAPFISDIQLKNESDEESTLSFLLHFQGSPS 138
TVAG_302900/Mmm1c-like   SLEFNEIE--------IKEVPPEISQAIIT-ETKFSEFVTLKCFYKPEMV 133
TVAG_139550/Mmm1b-like   YFKLNSIG--------SNPIISHISTLKMKEAD--------------DIR 74
TVAG_194830/Mmm1a-like   KFELLTLG--------NSPVIPYVATLDVNNKD--------------DIK 78

TVAG_214860/Mmm1         ISIAAT--VSAGPIDIPQLFSFHMKVELILCLLVARVTIKFKNDKSKEIS 186
TVAG_302900/Mmm1c-like   ISALSTVSVSILP-------SFNLGIDAKLNQIDADIALGIPESK~GDAY 175
TVAG_139550/Mmm1b-like   IAVPIT--LDIGPSFDVGFNCKNLILKIDVIKLKTTLLLTWLGNSDTCIE 122
TVAG_194830/Mmm1a-like   ILIPLT--WEEGPSLNFSMLNENLTAEVDLKLFKGTLLVSWPTNQEIDLE 126

TVAG_214860/Mmm1         VCIGNDLIIDINVK----------------------------------- 200
TVAG_302900/Mmm1c-like   IQMQNSTSVNFDVGASVKFVSINTEYL--GPVWTS-LREAVNYIIRSIKI 222
TVAG_139550/Mmm1b-like   LTFVDGFDIDFYLS--VKLFHFLTFTLSEIPILGAIIKALGTLFIQRQVI 170
TVAG_194830/Mmm1a-like   IRFINDCKIDFDVS--LILFKNTWLPLSSIPLFGPVIKGLISFFMTKGAI 174

TVAG_214860/Mmm1         ----------------------------------------~PLLDDP 206
TVAG_302900/Mmm1c-like   KIPLEQALTNEEEEEKEEEEAKEEEKKQLPRNDSTHEVIEIHPVPVKSDV 272
TVAG_139550/Mmm1b-like   KINLPKPVTRESLQQFY---------------------------------- 187
TVAG_194830/Mmm1a-like   KVKAEIQIPDELR------------------------------------- 186

TVAG_214860/Mmm1         KNASQKHIESISTWFSNFAIMSLRGKTFNIPVQ 239
TVAG_302900/Mmm1c-like   KVIID-------PIFKSYQL------------- 285
TVAG_139550/Mmm1b-like   ---------------------------------- 187
TVAG_194830/Mmm1a-like   ---------------------------------- 187
```

Figure 34. Protein sequence alignment of *T. vaginalis* Mmm1 and Mmm1-like proteins. Conserved region is marked in green. Conserved region in Mmm1 is located at 52-75 AA position, in Mmm1c-like at 53-75 AA, in Mmm1b-like at 10-34 AA and in Mmm1a-like at 14-37 AA.

Search for SMP domain using Interproscan were negative for all Mmm1-like proteins. SMP are characteristic with 6-β-strands and 3 helices to form a barrel (Schauder et al., 2014). They can form homo- or heterodimers. Therefore, we attempted to predict secondary structure of Mmm1 proteins using SWISS-MODEL protein structure homology-modelling server (Fig. 35).

The searches for suitable template revealed either Mmm1 model 5yk6.1 or Extended synaptotagmin-2 model 4p42.1.A.

Mmm1 *Zygosaccharomyces*

Template 5yk6.1.A

Homodimer, α4 and β6

GMQE 0,52

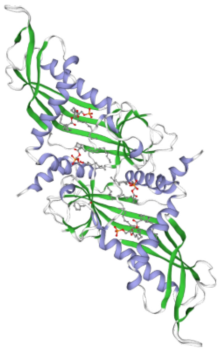

TV Mmm1

Template 5yk6.1.A

Homodimer, α2 and β8

GMQE 0,34

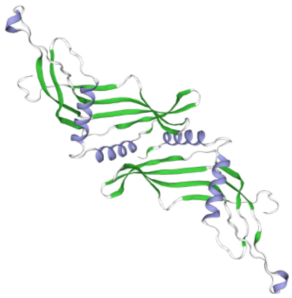

TV Mmm1a-like

Template 4p42.1.A

Monomer, α2 and β6

GMQE 0,20

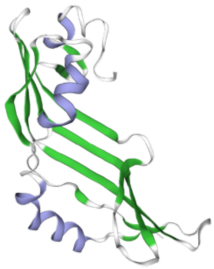

Tv Mmm1b-like

Template 4p42.1.A

Monomer, α2 and β8

GMQE 0,41

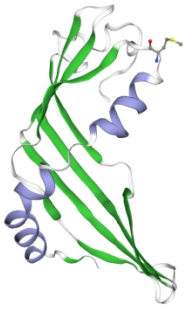

Tv Mmm1c-like

Template 4p42.1.A

Homodimer, α2 and β6

GMQE 0,20

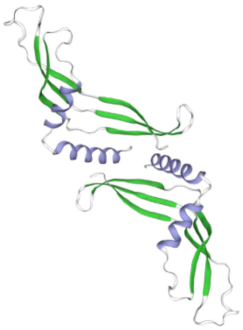

Figure 35. Prediction of Mmm1 and Mmm1-like protein structure using SWISS-MODEL protein structure homology-modelling server. GMQE - Global Model Quality Estimation (range 0-1). Beta sheets in green, alpha helices in purple.

All Mmm1-like proteins share similar SMP domains with tunnel-like structure as Mmm1 of *T. vaginalis* and of *Z. rouxii*. However, *T. vaginalis* Mmm1 and Mmm1-like proteins possess only 2 α-helices whereas SMP of *Z. rouxii* Mmm1 contains 4 α-helices. In addition, only Mmm1 and Mmm1c-like protein of *T. vaginalis* possess N-terminal TMD, whereas TMD is absent in Mmm1a and Mmm1b-like proteins.

5.4.2 Immunoprecipitation of Mmm2b and Mdm12

The same IP protocol was used for IP of Mmm2b and Mdm12. To verify successful IP, we analyzed samples with SDS-PAGE and Western blotting and monitored Mmm2b and Mdm12 during IP steps (Fig. 36).

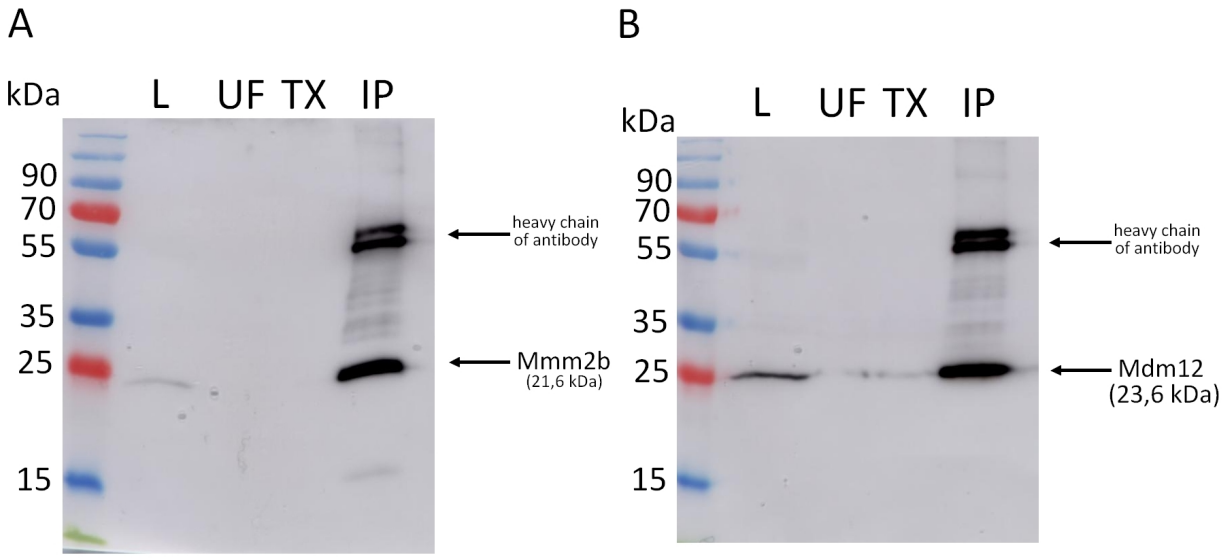

Figure 36. Western blot analysis of Mmm2b (A) and Mdm12 (B) IP.
IP was performed using DSP treated cells. During IP we tested protein fractions for presence of HA-tagged protein. L – cell lysate, UF – unbound fraction (sample of protein that did not bind to dynabeads), TX - sample of cells that were treated with Triton X–100, IP – immunoprecipitated proteins.

We performed IP in triplicates with Mmm2b-HA, Mdm12-HA recombinant proteins and wild type cells as control. IP proteins were submitted to quantitative mass spectrometry. The Mmm2b IP proteome dataset contained 1291 (Table 3-B in supplementary data at CD disk). Mdm12 IP proteome dataset contained 1290 proteins (Table 3-C in supplementary data at CD disk). LFQ intensities for all proteins identified for Mmm2b, Mdm12 cell lines and control cells were used as input data for Perseus software to test statistical support for co-immunoprecipitated proteins as for Mmm1. Multi-scatter plot (Fig. 37) revealed that the data are more consistent in comparison to Mmm1 dataset (Pearson coefficient range 0,726-0,95).

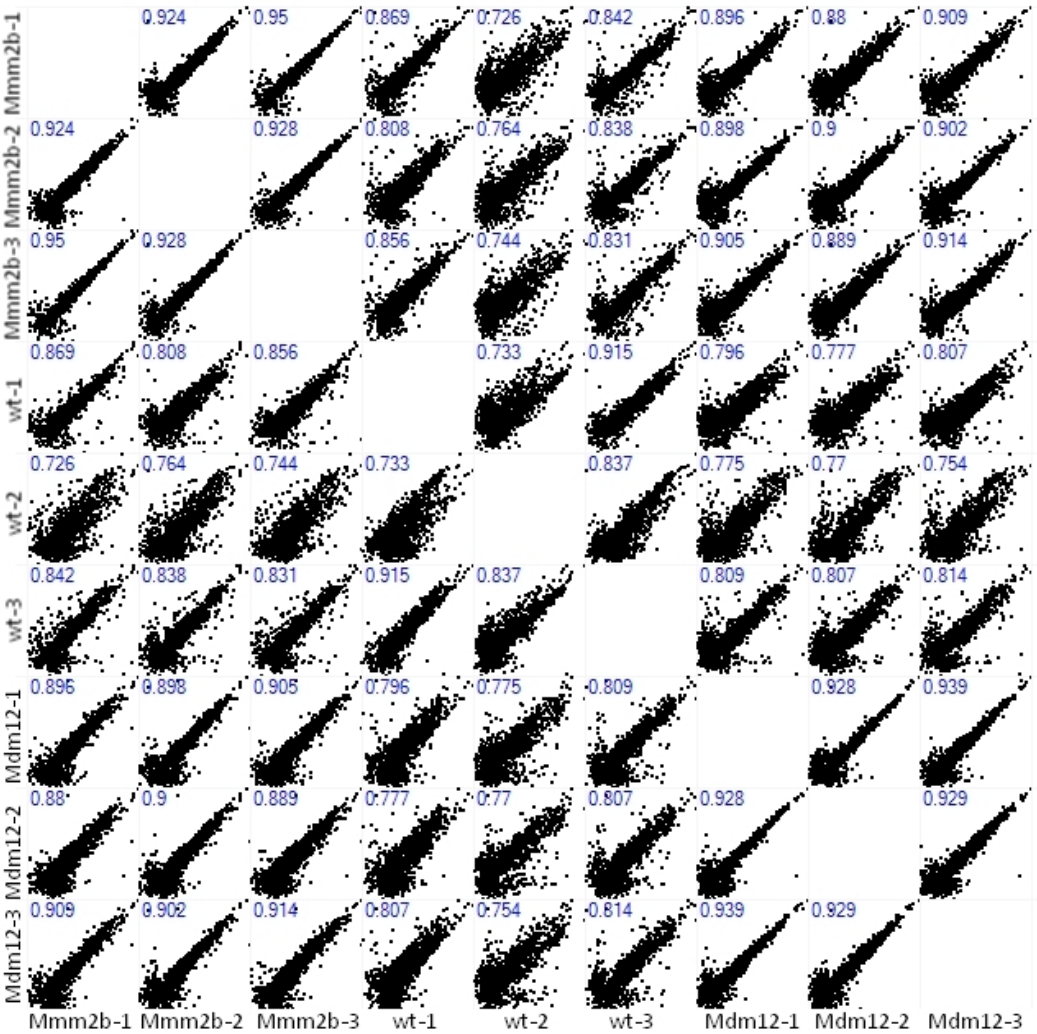

Figure 37. Multi-scatter plot analysis of data obtained for triplicates of Mmm2b (Mmm2b-1, Mmm2b-2, Mmm2b-3) and Mdm12 (Mdm12-1, Mdm12-2, Mdm12-3) against each other and

against data for triplicate of controls (wt-1, wt-2, wt-3). Numbers in the left upper corner represent the value of Pearson coefficient

In the next step, we constructed Volcano plot for Mmm2b and Mdm12 datasets that revealed 53 and 115 proteins, respectively with statistical support to be co-immunoprecipitated with corresponding HA-tagged recombinant proteins (Fig. 38 and 39).

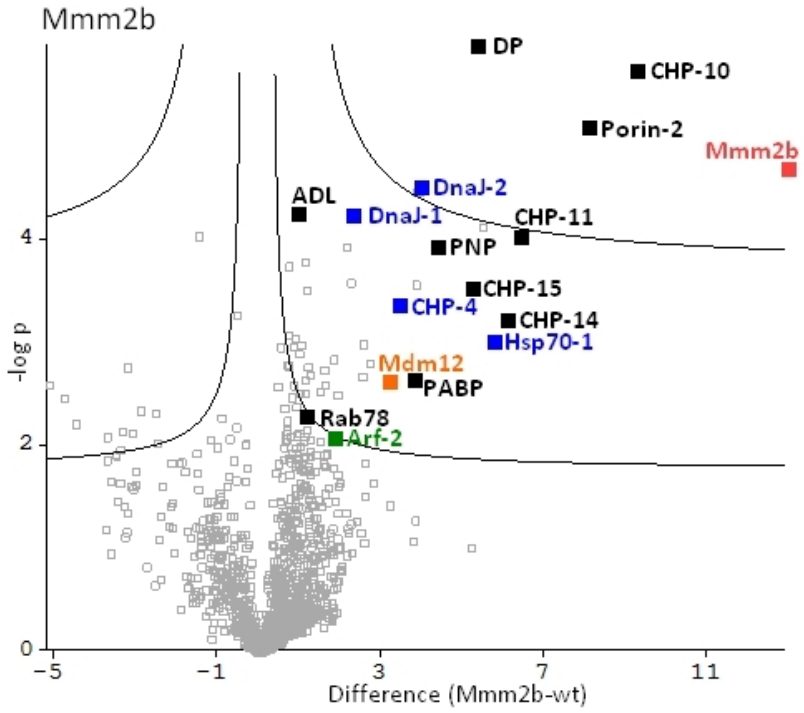

Figure 38. Volcano plot displaying significant proteins that co-immunoprecipitated with Mmm2b with significant statistical support (s0=0,1 and FDR=0,05). Black squares represent proteins that co-immunoprecipitated also with Mdm12 (Fig. 39). Blue squares represent proteins that co-immunoprecipitated with Mmm2b, Mmm1 and Mdm12. Green square represents protein that co-immunoprecipitated with Mmm2b and Mmm1. Red square represents Mmm2b. Orange square represents Mdm12.

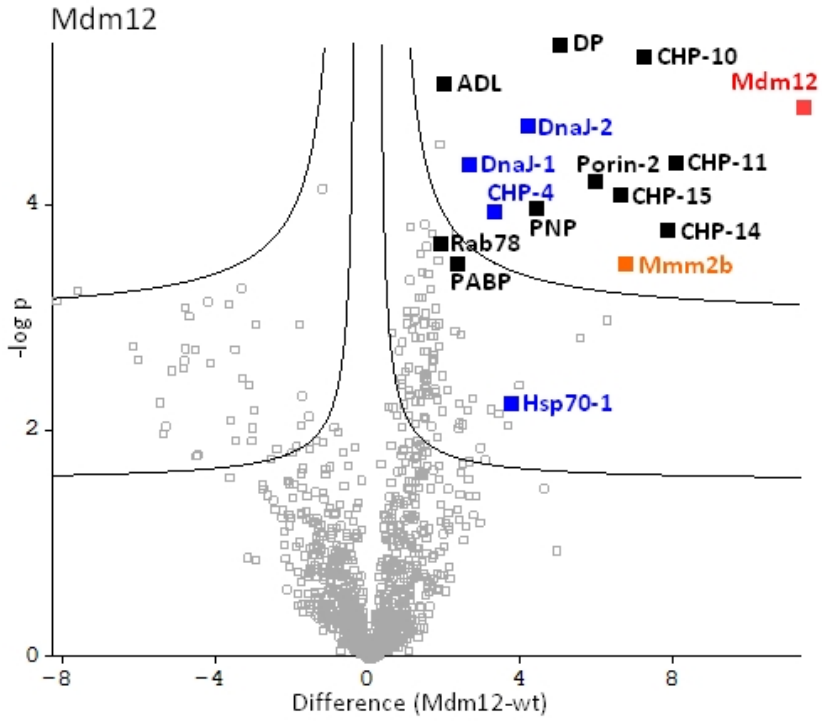

Figure 39. Volcano plot displaying significant proteins that co-immunoprecipitated with Mdm12 with significant statistical support (s0=0,1 and FDR=0,05). Black squares represent proteins that co-immunoprecipitated also with Mmm2b (Fig. 38). Blue squares represent proteins that co-immunoprecipitated with Mdm12, Mmm1 and Mmm2b. Red square represents Mdm12. Orange square represents Mmm2b.

To compare datasets of proteins co-immunoprecipitated with Mmm2 and Mdm12, we used “Hawaii plot” tool in Perseus software that allows construction and comparison of multiple volcano plots. This analysis revealed 35 proteins that are common to Mmm2b and Mdm12 dataset (Table 5, Table 5 in supplementary data at CD disk). Hawaii plot allows to set two cut-off thresholds. Significance A with FDR=0,01 and more stringent significance B where FDR=0,05. Proteins above significance A are considered the best candidates for putative interactors. Most importantly, we identified Mdm12 protein in Mmm2 dataset above significance B and vice versa, which indicates interaction between these two proteins.

We also compared Mmm1 dataset with Mmm2b and Mdm12 and we identified 4 proteins common to both Mmm2b and Mdm12 data (Table 4) and another 4 only to Mdm12 data (Table 4).

Proteins listed in Table 5 were analyzed by wide range of bioinformatic tools. We searched for conserved domains (Interproscan), transmembrane domains (TmHMM), cell localization (PSORTII) and signal peptides (TargetP). We used NCBI BLAST and HHpred for protein homology searches.

Table 5. *In silico* analysis of co-immunoprecipitated proteins common to Mmm2b and Mdm12.

	Label	Protein name	Accession number	Interproscan (domain)	TmHMM	PSORTII	TargetP	NCBI	HHpred
FDR 0,01	**Mmm2b**	Mmm2b	**TVAG_375920**	SMP	0	cytoplasmic	no	Mdm34	Mdm34
	Mdm12	Mdm12	**TVAG_063000**	SMP	0	cytoplasmic	no	no hint	Mdm12
	Porin-2	Porin-2	**TVAG_340380**	no hint	0	cytoplasmic	no	no hint	Tom40
	DnaJ-2	DnaJ-2	**TVAG_317210**	Hsp40/DnaJ	0	cytoplasmic	no	DnaJ	DnaJ
	DnaJ-1	DnaJ-1	**TVAG_305730**	Hsp40/DnaJ	0	nuclear	no	DnaJ	DnaJ
	PNP	purine nucleoside phosphorylase	**TVAG_454490**	nucleoside phosphorylase	0	cytoplasmic	no	purine nucleoside phosphorylase	purine nucleoside phosphorylase
	PABP-2	polyadenylate-binding protein	**TVAG_278520**	RNA recognition motif domain	0	nuclear	no	polyadenylate-binding protein	polyadenylate-binding protein
	Rab78	Rab78	**TVAG_159730**	small GTP-binding protein	0	cytoplasmic	M	small GTP-binding protein	ras related protein
	ADL	AMP dependent ligase	**TVAG_340550**	AMP-dependent synthetase/ligase	0	cytoplasmic	no	AMP-binding enzyme family protein	long-chain-fatty-acid-CoA ligase
	DP	Dullard protein	**TVAG_274690**	FCP1 homology domain	0	nuclear	no	NLI interacting factor-like phosphatase family protein	TIM50
	CHP-4	cysteine protease	**TVAG_514800**	cysteine protease	0	nuclear	no	cysteine protease	myeloid leukemia factor
	CHP-11	conserved hypothetical protein	**TVAG_454360**	EF-hand domains	0	cytoplasmic	no	EF-hand family protein	EF-hand calcium binding domain protein
	CHP-14	conserved hypothetical protein	**TVAG_020600**	myeloid leukemia factor	0	nuclear	no	glycine-rich protein	myeloid leukemia factor
	CHP-10	conserved hypothetical protein	**TVAG_197670**	mitochondrial carrier	1	nuclear	no	no hint	calcium-binding mitochondrial carrier protein
	CHP-15	conserved hypothetical protein	**TVAG_290210**	EF-hand domains	0	cytoplasmic	no	EF-hand family protein	EF-hand calcium binding domain protein
FDR 0,05	**CHP-13**	conserved hypothetical protein	TVAG_150300	myeloid leukemia factor	0	nuclear	no	glycine-rich protein	myeloid leukemia factor
	CHP-16	conserved hypothetical protein	TVAG_106520	PTHR42649:SF34 domain	0	cytoplasmic	no	no hint	BTB/POZ domain
	CHP-17	conserved hypothetical protein	TVAG_353990	deoxynucleoside kinase domain	0	cytoplasmic	no	deoxynucleoside kinase	deoxynucleoside kinase
	CHP-19	conserved hypothetical protein	TVAG_298130	EF-hand domains	0	nuclear	no	EF-hand family protein	EF-hand family protein

	Hsp70-1	Hsp70-1	TVAG_291920	Hsp70/DnaK	0	nuclear	no	DnaK	Hsp70
	Hsp70-2	Hsp70-2	TVAG_479220	Hsp70 domain	0	nuclear	no	DnaK	Hsp70
	Hsp70-4	Hsp70-4	TVAG_423170	armadillo-type fold	0	ER	no	no hint	no hint
	DnaJ-3	DnaJ-3	TVAG_347420	DnaJ domain	0	nuclear	no	DnaJ	DnaJ
	Rab5	Rab5	TVAG_121740	small GTP-binding protein	0	cytoplasmic	no	ras family protein	EF-hand domain ras family related protein
	Rab6	Rab6	TVAG_580280	small GTP-binding protein	0	nuclear	no	small GTP-binding protein	ras related protein
	Rab8	Rab8	TVAG_282070	small GTP-binding protein	0	cytoplasmic	SP	small GTP-binding protein	ras related protein
	Rabx21	Rabx21	TVAG_211200	small GTP-binding protein	0	cytoplasmic	no	small GTP-binding protein	ras related protein
	Rab21	Rab21	TVAG_065320	small GTP-binding protein	0	cytoplasmic	no	small GTP-binding protein	EF-hand domain ras family related protein
	Rab19.41	Rab19.41	TVAG_181000	small GTP-binding protein	0	cytoplasmic	no	small GTP-binding protein	ras related protein
	Rab32	Rab32	TVAG_379850	small GTP-binding protein	0	cytoplasmic	no	GTP-binding protein YPTM1	ras related protein
	G-α	G-protein α subunit	TVAG_274750	G-protein α subunit	0	nuclear	no	G-protein α subunit	G-protein α subunit
	Hmp35	hydrogenosomal membrane protein 35	TVAG_590550	no hint	0	cytoplasmic	no	hydrogenosomal membrane protein 35	VDAC
	T-complex-1	T-complex protein 1	TVAG_137820	T-complex protein 1	0	cytoplasmic	no	chaperonin subunit delta CCTdelta	chaperonin-containing T-complex
	α-tub	α-tubulin 1	TVAG_467840	alpha tubulin	0	cytoplasmic	no	alpha-tubulin 1	tubulin alpha
	DoxR	disulfide oxidoreductase	TVAG_049830	FAD/NAD(P)-binding domain; Flavodoxin/ nitric oxide synthase	0	cytoplasmic	no	A-type flavoprotein	no hint
	actin3	actin	TVAG_485210	actin	0	cytoplasmic	no	actin	actin
	U1	ubiquitin	TVAG_184180	ubiquitin	0	cytoplasmic	no	polyubiquitin	ubiquitin

Proteins with FRD=0,01 are in blue part of the table. Proteins with FDR=0,05 are in orange part of the table. All 9 conserved hypothetical proteins (CHP) are in grey. Proteins that are common to Mdm12, Mmm2b and Mmm1 (4) are depicted in green. SP – secretory pathway, M – mitochondrion.

Detected CHP contained calcium-binding protein, 2 EF-hand domain (with helix-loop-helix motif) proteins, 2 glycine-rich proteins and protein of unknown function with predicted POZ (Pox virus and Zinc finger) domain. We also identified 6 heat shock proteins, 8 ras related proteins, purine nucleoside phosphorylase, polyadenylate-binding protein, porin-2 and hydrogenosomal membrane protein 35 (Hmp35).

When we compared volcano plots for Mmm2b and Mdm12, we identified several proteins that were significantly enriched for Mmm2 but under the cut-off line in Mdm12 dataset (Fig. 40, Table 6 in supplementary data at CD disk) and vice versa (Fig. 41, Table 7 in supplementary data at CD disk).

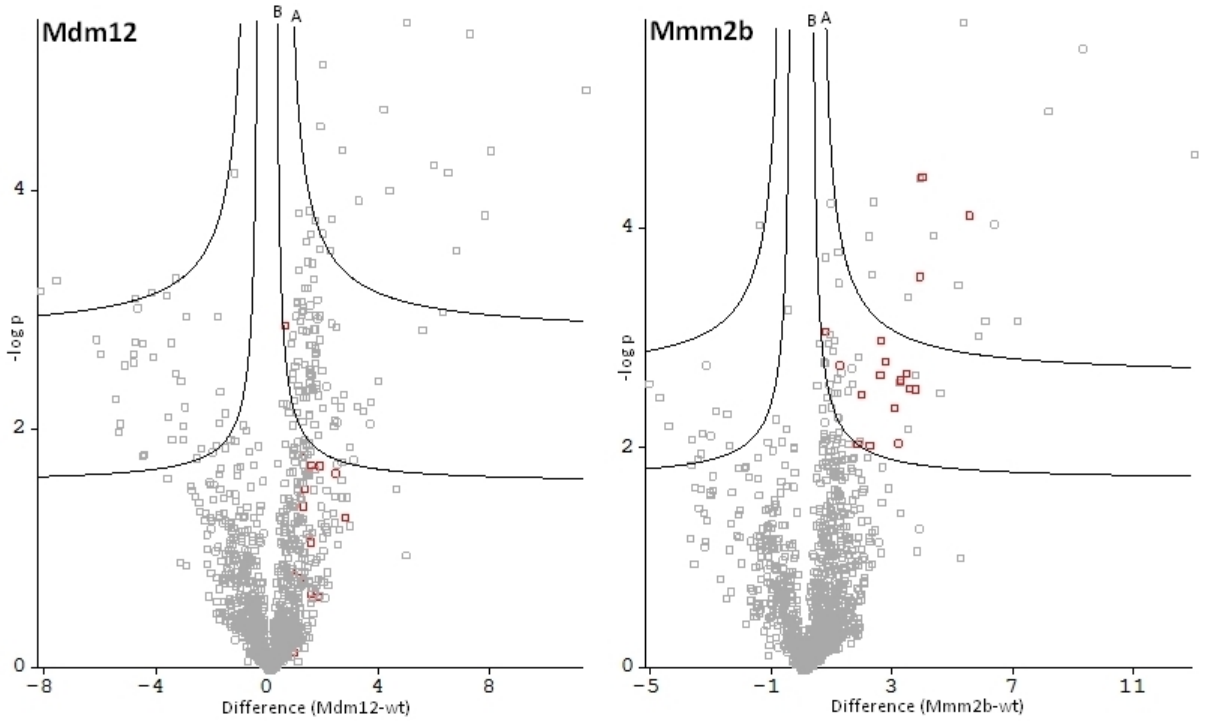

Figure 40. Volcano plot displaying significant proteins that co-immunoprecipitated with Mmm2b with significant statistical support (s0=0,1 and FDR=0,05), but in Mdm12 data under the significance cut-off. Red dots highlight individual proteins.

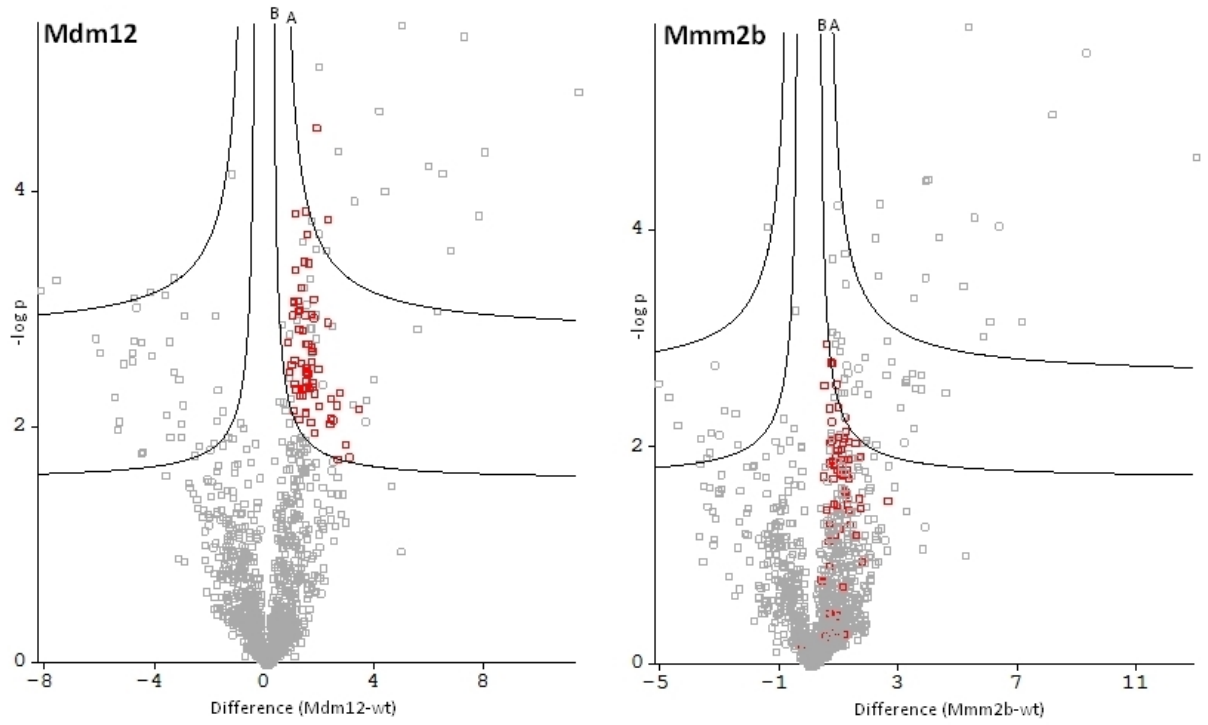

Figure 41. Volcano plot displaying significant proteins that co-immunoprecipitated with Mdm12 with significant statistical support (s0=0,1 and FDR=0,05), but in Mmm2b data under the significance cut-off. Red dots highlight individual proteins.

Statistically supported proteins that are present in Mmm2b dataset but missing in statistically supported Mdm12 dataset contain 6 CHP (deoxynucleoside kinase, EF-hand domain containing protein, 2 importin β proteins). Bioinformatical analysis of the remaining CHP like CHP-18, CHP-22 and CHP-24 did not bring any insight into their function. Statistically enriched proteins include wide range of ras related proteins (8) and proteins with other functions (15) like thioredoxin, peroxiredoxin and A-type flavoprotein.

Statistically supported proteins that are present in Mdm12 dataset but missing in Mmm2b dataset contain 8 CHP (from which 3 are EF-hand domain containing proteins and CHP-9/Mmm1c-like protein). Statistically enriched proteins include wide range of GTP-binding proteins (40) and proteins with other functions (21) like chaperonins, adenosine deaminase and synaptojanin.

To summarize previous data, we visualized the interacting proteins in interaction network using Cytoscape software (Fig. 42).

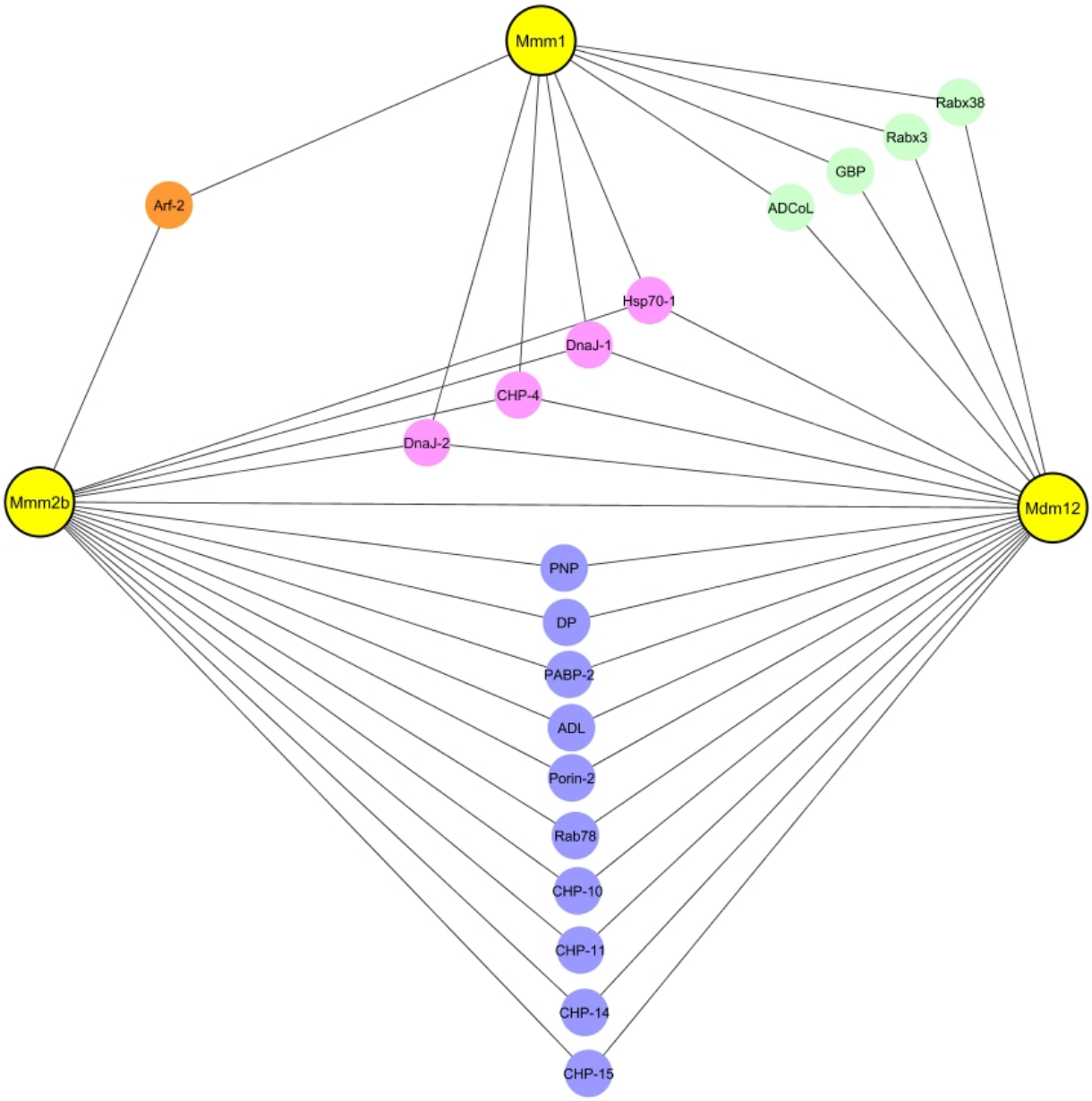

Figure 42. Protein interaction network

The interactome includes 14 proteins that are common to Mmm2b and Mdm12 (blue, FDR=0,01), 4 proteins common to Mmm2b, Mdm12 and Mmm1 (pink), 4 proteins common to Mmm1 and Mdm12 (green) and 1 protein that interacts with Mmm1 and Mmm2b (orange). Proteins abbreviations are according to Table 4 and 5.

6. DISCUSSION

ERMES, a structure that mediates interaction between mitochondria and ER, was initially found in fungi (Kornmann et al., 2009). Following *in silico* analyses predicted presence of ERMES in some lineages of eukaryotic supergroups Opisthokonta, Amoebozoa and Excavata whereas ERMES seems to be absent in Archaeplastida and SAR (Wideman et al., 2013). ERMES is also absent in organisms with reduced mitochondria of mitosome type such as Giardia and Entamoeba (Wideman et al., 2013). Presence of ERMES in organisms with hydrogenosomes is unclear. Incomplete set of highly divergent ERMES components Mmm1, Mmm2 and Mdm12 was found in the genome of *T. vaginalis* that harbor hydrogenosomes (Wideman et al., 2013). However, no experimental evidence is available in support of the predicted function. Our initial homology searches in *T. vaginalis* genome revealed presence of two Mmm2 paralogs (Mmm2a and Mmn2b) and single copy genes for Mmm1 and Mdm12. However, no homolog of Mdm10 was identified. Bioinformatic analyses of *T. vaginalis* ERMES components showed similar characteristics with fungal orthologs. Cell localization studies demonstrated that Mmm1 is ER bound protein and Mmm2 is associated with outer hydrogenosomal membrane. Investigation of ERMES components interactions supported expected interactions between Mmm2 and Mdm12. However, we did not find convincing evidence for interactions between Mmm1 and other components. Immunoprecipitation of protein complexes and quantitative mass spectrometry identified new possible interacting partners to ERMES. Most interestingly, hydrogenosomal protein porin-2 immunoprecipitated with Mmm2 and Mdm12 and appeared as the best candidate to substitute the function of absent component Mdm10. We also identified three Mmm1-like proteins with SMP domains, however its role in lipid transport needs to be clarified.

6.1 *In silico* analysis of ERMES components

Our searches for homologs of ERMES in *T. vaginalis* genome confirmed presence of Mmm1, Mmm2 and Mdm12, although they are highly divergent from known orthologs. Moreover, we found that Mmm2 is present in two paralogs (Mmm2a and Mmm2b). All ERMES subunits contain SMP domains that act as tethers in membrane contact sites. SMP domains are also present in extended-synaptotagmin proteins such as tricalbin (Reinisch et al., 2016). SMP domains form barrel-like structures that can bind various types of glycerophospholipids, e.g.

phosphatidylcholine (AhYoung et al., 2015; Reinisch et al., 2016). Interestingly, bioinformatic analysis of conserved hypothetical proteins that co-immunoprecipitated with Mmm1 and following searches in *T. vaginalis* genome pointed out on three proteins with homology to Mmm1 named: Mmm1a-like, Mmm1b-like and Mmm1c-like proteins. Prediction of their structure using SWISS-MODEL server showed that all Mmm1-like proteins share similar tunnel-like structure as Mmm1 of *T. vaginalis* and of *Z. rouxii* that is characteristic for tubular-lipid binding (TULIP) protein superfamily to which proteins with SMP domain belong. However, only Mmm1 and Mmm1c-like protein of *T. vaginalis* possess N-terminal TMD that anchors Mmm1 to ER membrane. Moreover, *T. vaginalis* Mmm1 and Mmm1-like proteins possess only 2 α-helices whereas SMP of *Z. rouxii* Mmm1 contain 4 α-helices. Therefore, it is difficult to estimate, which of four *T. vaginalis* Mmm1 candidates function in lipid transport to the hydrogenosomal membranes as Mmm1 and which transport lipids to membranes of other destinations as synaptotagmins (Schauder et al., 2014).

6.2 Cellular localization of ERMES in *T. vaginalis*

Fungal Mmm1, Mmm2 and Mdm12 are known to reside in ER, outer mitochondrial membrane and the cytosol, respectively (Kornmann et al., 2009). Because of high divergence of putative ERMES orthologs in *T. vaginalis*, it was important to test whether their cell localization corresponds to expected cellular localization. Immunofluorescence microscopy revealed presence of Mmm1 in structures corresponding to ER and co-localized with ER marker protein SPDI. Proteomic data revealed proteins predicted to localize in ER and number of ras related proteins from Rab subfamily that are involved in vesicle trafficking. Therefore, we suggest that Mmm1 is bound to ER membrane facing the cytosol interacting with cytosolic proteins.

Mmm2 is a mitochondrial outer membrane protein (Youngman et al., 2004). IF microscopy showed that Mmm2a and Mmm2b form small dots with similar overall distribution as hydrogenosomes. Super-resolution microscopy revealed that these dots are present in discrete domains on the hydrogenosomal membrane, or in close proximity to hydrogenosomes. Cell fractionation by differential centrifugation showed that Mmm2 is associated with hydrogenosomes but might be present also in other cellular compartments such as LDV and

cytoplasm. These phenomena might be caused by the over expression of tagged protein or contamination of LDV with hydrogenosomes as there was no form of control. This control should consist of cytosolic protein and hydrogenosomal protein. The protein protection assay revealed that Mmm2 is not protected by hydrogenosomal membranes. *In silico* prediction did not identify any transmembrane domain in Mmm2. Therefore, Mmm2 seems to be loosely associated with outer hydrogenosomal membrane facing cytosol via unclear mechanisms. Association of Mmm2 with mitochondrial membrane is a matter of discussion. It has been reported that Mmm2 resides in the membrane via beta-sheet conformation (Youngman et al., 2004). However, more recent studies suggested that Mmm2 is not integral membrane protein but it is peripherally attached to the outer mitochondrial membrane via binding to Mdm10, which serves as integral membrane anchor for ERMES (Ellenrieder, et al., 2016).

Similar punctuate pattern of labeling on hydrogenosomes was observed for Mdm12. It is likely that labeled discrete domains represent membrane contact sites between hydrogenosomes and possibly ER. Similar pattern has been observed for yeast mitochondria where Mdm12 was distributed in numerous (10-15) discrete foci within mitochondria (Berger et al., 1997). On the other hand different publications display Mdm12 only as a few (3-7) punctuate dots (Kornmann et al., 2009) (Boldogh et al., 2003).

Hydrogenosomal localization of Mmm2/Mdm12 is further supported by identification of porin-2 among interacting partners. Porin-2 is a hydrogenosomal membrane protein (Rada et al., 2011). Other hydrogenosomal membrane proteins such as Hmp-35-1 (Dyall et al., 2003), Hmp-36-2 (Rada et al., 2011) and C-tail-6 were detected in proteomic data, however support for their association with Mmm2b was under the cut off for the statistical significance.

6.3 Porin-2: A possible substitute for subunit Mdm10

Mdm10 is a β-barrel protein (Flinner et al., 2013) that is one of the core components in ERMES complex (Kornmann et al., 2009). Mdm10 is integrated into the lipid phase of outer mitochondrial membrane and serves as an integral membrane anchor for Mmm2. Moreover, Mdm10 is required for biogenesis of SAM and Tom40 (Ellenrieder et al., 2016). However *mdm10* gene was not found in the genome of *T. vaginalis* by us as well as previous studies using homology searches (Wideman et al., 2013). Noteworthy, we identified β-barrel protein named porin-2 as an interacting partner for both Mmm2b and Mdm12. Porin-2 was previously detected in the proteome of hydrogenosomal membranes (Rada et al., 2011). As other β-barrel proteins, porin-2 contains C-terminal beta signal (Rada et al., 2011) and is formed by 18 transmembrane beta strands. Similar structure is known for Tom40 component of translocase of outer membrane (TOM) and voltage-dependent anion channels (VDAC). However, porin-2 appeared to be too divergent to be aligned with the TOM or VDAC sequences. Moreover, current investigation of *T. vaginalis* Tom40 did not suggest any relationship between Tom40 and porin-2 (Makki et al., 2019) nor there is any interaction with SAM. In contrast, immunoprecipitation of Mmm2b and Mdm12 revealed statistically well supported interaction with porin-2. Thus, porin-2 is a strong candidate that may functionally replace Mdm10. Further investigation is required to test this hypothesis.

6.4 GTPases Gem1 and Arf1

The function of ERMES complex is regulated by Miro GTPase Gem1 (Kornmann et al., 2011). Gem1 affects the size and occurrence of ERMES in the cell (Kornmann et al., 2011). Although we identified over 40 small GTPases in the list of putative interacting partners for ERMES subunits, we did not identify any protein that would conform to be Miro GTPase.

Arf1 is a small GTPase that is known as a key factor for the recruitment of the COPI coat proteins to the Golgi membrane. Arf1 exists in a GDP-bound form that is associated with membranes and as a GTP-bound form that is present in the cytosol (Donaldson et al., 2011). More recently, the second role of Arf1 was identified as a regulator of the morphological and functional maintenance of mitochondria. Arf1 facilitate correct recruitment of mitophagy components to clear damaged mitochondria. It has been shown that Arf1 functionally localizes to

ERMES contact sites (Rabouille, 2014) and regulates ERMES formation (Zhang et al., 2018). *T. vaginalis* as well as mammalian cells or yeast remove old or damaged hydrogenosomes in the process of autophagy (Benchimol, 1999). Immunoprecipitation of Mmm1, Mmm2b and Mdm12 revealed association of two Arf proteins from which one (accession number TVAG_262220) has been found in all immunoprecipitated samples and shares 59,1 % protein sequence similarity with Arf1. Therefore, further investigations are needed to verify whether this Arf homolog plays a role in ERMES regulation.

6.5 Interaction of ERMES subunits

We attempted to verify interactions between ERMES components of *T. vaginalis* due to their significant divergence from known orthologs. Mmm2b and Mdm12 proteins co-immunoprecipitated with each other and that strongly supports interaction between these two ERMES components. In addition, proteomic data have shown 35 proteins that were co-immunoprecipitated with Mmm2b and Mdm12 with statistically significant support. Investigations of interaction between Mmm1 and Mmm2b using IF microscopy revealed only a few colocalizing dots or dots in close proximity that might suggest interaction between these two proteins. However, Mmm1 was immunoprecipitated with neither Mmm2b nor Mdm12. These results suggest that Mmm1 and Mmm2b/Mdm12 form only transient interactions. Indeed, similar observation was reported in the study of ERMES in yeast. It has been shown that Mmm2b can be efficiently immunoprecipitated from Triton X-100 or digitonin extract of mitochondrial proteins, however Mmm1 does not co-precipitate with Mmm2 (Youngman et al., 2004). Furthermore, Mmm1 and Mmm2 co-localize only in few discrete foci and appear to be part of two separate complexes. Interaction between these two complexes seems to be rather dynamic, not stable (Youngman et al., 2004). We suggest that interaction between Mmm1 and Mmm2b/Mdm12 is similarly dynamic, while Mmm2b and Mdm12 form a more stable complex. Noteworthy, Mmm1 immunoprecipitated with two Mmm1-like proteins (Mmm1a-like and Mmm1c-like). Mmm1b-like TVAG_139550 was also identified but under the cut-off of Volcano statistical support. We can hypothesize that Mmm1-like proteins may interact with Mmm1 and form a separate complex(s) at ER membrane. Moreover, Mmm1c-like protein was co-immunoprecipitated with Mdm12. These observations need to be further investigated. However, we cannot exclude a

possibility that inability to pull down Mmm1 with other ERMES components might be caused by non-optimal experimental conditions. Therefore, in future experiments, we will attempt to adjust experimental conditions e.g. to test more detergents used for permeabilization of membranes and various buffers. We will also need to establish new methods such as use of fusion tags in fluorescence microscopy.

6.6 Phosholipid trafficking via ERMES

The key role of ERMES is phospholipid transport between ER and mitochondria (Kornmann et al., 2009). Phospholipids bind to SMP domains of ERMES proteins - Mmm1, Mmm2 and Mdm12. Phospholipids are then transported via these proteins from ER to mitochondria, although mechanism is not fully understood (Endo et al., 2018). All ERMES components that are present in *T. vaginalis* contain SMP domain, which suggests their possible involvement in phospholipid transfer between ER and hydrogenosomes as in yeast between ER and mitochondria (Kojima et al., 2016). Proteomic dataset of immunoprecipitated proteins contain some proteins that are involved in phospholipid biosynthesis (such as acetyltransferase), however their association with phospholipid transfer via ERMES components is not statistically supported. Phospholipid transfer between ERMES components in *T. vaginalis* needs to be further investigated. However, to obtain the evidence of phospholipid trafficking is experimentally challenging.

6.7 Other ERMES functions

Apart from phospholipid trafficking and maintenance of mitochondrial morphology, ERMES is involved in regulation of iron homeostasis. Impaired ERMES complex causes defect in mitochondrial protein import, which results in disrupted iron–sulfur cluster biosynthesis, inducing the iron deficiency response, slow growth and loss of mtDNA (Xue et al., 2017). *T. vaginalis* is an organism that is highly dependent on iron-sulfur proteins. Iron-sulfur clusters (FeS) are synthesized in hydrogenosomes (Tachezy & Doležal, 2007). We did not find any direct proof of ERMES involvement in iron homeostasis. However, this topic could be an interesting subject of future studies.

In trichomonads, hydrogenosomes contain intermembrane vesicle which stores calcium (Benchimol, 2000). We identified several calcium-binding proteins with EF-hand domain that immunoprecipitated with Mmm1, Mmm2 and Mdm12. Proteins containing EF-hand domains may maintain homeostasis of calcium in cytosol, possibly in hydrogenosomes or transduct signal between organelles (Skelton et al., 1994). Therefore, the presence of these proteins suggests possible link of ERMES to calcium homeostasis.

7. CONCLUSIONS AND PERSPECTIVES

This thesis was focused on ERMES components in *T. vaginalis*. Main goals were to establish cellular localization of these components and to investigate possible interactions between them. We demonstrated the hydrogenosomal localization of Mmm2b and we also prove that Mmm2b and Mdm12 are interacting partners. In addition, we provided evidence that Mmm1 is associated to ER. We suggest that Mmm1 can interact with other ERMES components transiently. Moreover, we discovered new possible interaction partners, namely porin-2, which could functionally substitute missing component Mdm10, and three divergent Mmm1-like proteins. Our results also bring a lot of new questions.

1. What is the function of ERMES in *T. vaginalis*?
2. Does porin-2 substitute the function of Mdm10?
3. Is there a functional difference between Mmm2a and Mmm2b?
4. What is the role of Mmm1-like proteins?
5. What is the role of Arf1 and is there Gem1?
6. Is there any role of other interacting partners for ERMES complex?

8. LITERATURE

Ackema, K. B., Spang, A., Hench, J., Böckler, S., Westermann, B., Wang, S. C., Frank, S., Sauder, U., Mergentaler, H., Bard, F., 2014. The small GTPase Arf1 modulates mitochondrial morphology and function. The EMBO Journal, *33*(22), 2659–2675.

AhYoung, A. P., Jiang, J., Zhang, J., Khoi Dang, X., Loo, J. A., Zhou, Z. H., Egea, P. F., 2015. Conserved SMP domains of the ERMES complex bind phospholipids and mediate tether assembly. Proceedings of the National Academy of Sciences, 112(25), 3179-3188.

Aiken Hobbs, A. E., Srinivasan, M., McCaffery, J. M., Jensen, R. E., 2001. Mmm1p, a mitochondrial outer membrane protein, is connected to mitochondrial DNA (mtDNA) nucleoids and required for mtDNA stability. Journal of Cell Biology, 152(2), 401–410.

Aurrecoechea C., 2009. GiardiaDB and TrichDB: integrated genomic resources for the eukaryotic protist pathogens *Giardia lamblia* and *Trichomonas vaginalis*.

Benchimol, M., Almeida, J. C. A., De Souza, W., 1996. Further studies on the organization of the hydrogenosome in *Tritrichomonas foetus*. Tissue and Cell, 28(3), 287-299.

Benchimol, M., 2000. Ultrastructural characterization of the isolated hydrogenosome in *Tritrichomonas foetus*. Tissue and Cell, 32(6), 518-526.

Benchimol, M., 1999. Hydrogenosome autophagy: An ultrastructural and cytochemical study. Biology of the Cell, 91(3), 165-174.

Berger, K. H., Sogo, L. F., Yaffe, M. P., 1997. Mdm12p, a component required for mitochondrial inheritance that is conserved between budding and fission yeast. Journal of Cell Biology, 136(3), 545–553.

Bertani, G., 1951. Studies on lysogenesis. I. The mode of phage liberation by lysogenic *Escherichia coli*. Journal of Bacteriology, 62(3), 293–300.

Boldogh, I. R., Nowakowski, D. W., Yang, H.-C., Chung, H., Karmon, S., Royes, P., Pon, L. A., 2003. A protein complex containing Mdm10p, Mdm12p, and Mmm1p links mitochondrial membranes and DNA to the cytoskeleton-based segregation machinery. Molecular Biology of the Cell, 14(11), 4618–4627.

Boldogh, I., Vojtov, N., Karmon, S., Pon, L. A., 1998. Interaction between mitochondria and the actin cytoskeleton in budding yeast requires two integral mitochondrial outer membrane proteins, Mmm1p and Mdm10p. The Journal of Cell Biology, 141(6), 1371–1381.

Burgess, S. M., Delannoy, M., Jensen, R. E.,1994. MMM1 encodes a mitochondrial outer membrane protein essential for establishing and maintaining the structure of yeast mitochondria. The Journal of Cell Biology, 126(6), 1375–1391.

CloneJET PCR Cloning Kit, Thermo Fisher Scientific, https://www.thermofisher.com/order/catalog/product/K1231

Cox, J., Hein, M. Y., Luber, C. A., Paron, I., Nagaraj, N., Mann, M., 2014. Accurate proteome-wide label-free quantification by delayed normalization and maximal peptide ratio extraction, termed MaxLFQ. Molecular & Cellular Proteomics : MCP, 13(9), 2513–2526.

Csordás, G., Renken, C., Várnai, P., Walter, L., Weaver, D., Buttle, K. F., Balla, T., Mannella, C. A., Hajnóczky, G., 2006. Structural and functional features and significance of the physical linkage between ER and mitochondria. The Journal of Cell Biology, 174(7), 915–921.

Delgadillo, M. G., Liston, D. R., Niazi, K., Johnson, P. J., 1997. Transient and selectable transformation of the parasitic protist *Trichomonas vaginalis*. Proceedings of the National Academy of Sciences, 94(9), 4716-4720.

Diamond, L. S., 1957. The establishment of various trichomonads of animals and man in axenic cultures. The Journal of Parasitology, 43(4), 488.

Dimmer, K. S., Fritz, S., Fuchs, F., Messerschmitt, M., Weinbach, N., Neupert, W., Westermann,

B., 2002. Genetic basis of mitochondrial function and morphology in *Saccharomyces cerevisiae*. Molecular Biology of the Cell, 13(3), 847–853.

Donaldson, J. G., Jackson, C. L., 2011. Arf family G proteins and their regulators: roles in membrane transport, development and disease. Nature Reviews Molecular Cell Biology, 12(6), 362–375.

Drmota, T., Proost, P., Van Ranst, M., Weyda, F., Kulda, J., Tachezy, J., 1996. Iron-ascorbate cleavable malic enzyme from hydrogenosomes of *Trichomonas vaginalis*: purification and characterization. Molecular and Biochemical Parasitology, 83(2), 221–234.

Dyall, S. D., Lester, D. C., Schneider, R. E., Delgadillo-Correa, M. G., Plümper, E., Martinez, A., Koehler, C. M., Johnson, P. J., 2003. *Trichomonas vaginalis* Hmp35, a putative pore-forming hydrogenosomal membrane protein, can form a complex in yeast mitochondria. Journal of Biological Chemistry, 278(33), 30548–30561.

Ellenrieder, L., Opaliłski, Ł., Becker, L., Krüger, V., Mirus, O., Straub, S. P., Ebell, K., Flinner, N., Stiller, S., Guiard, B., Meisinger, C., Wiedemann, N., Schleiff, E., Wagner, R., Pfanner, N., Becker, T., 2016. Separating mitochondrial protein assembly and endoplasmic reticulum tethering by selective coupling of Mdm10. Nature Communications, 7, 13021.

Endo, T., Tamura, Y., Kawano, S., 2018. Phospholipid transfer by ERMES components. Aging, 10(4), 528-529.

Flinner, N., Ellenrieder, L., Stiller, S. B., Becker, T., Schleiff, E., Mirus, O., 2013. Mdm10 is an ancient eukaryotic porin co-occurring with the ERMES complex. Biochimica et Biophysica Acta, 1833(12), 3314-3325.

Hebert, A. S., Richards, A. L., Bailey, D. J., Ulbrich, A., Coughlin, E. E., Westphall, M. S., Coon, J. J., 2014. The one hour yeast proteome. Molecular & Cellular Proteomics : MCP, 13(1), 339–347.

Helle, S. C. J., Kanfer, G., Kolar, K., Lang, A., Michel, A. H., Kornmann, B., 2013. Organization

and function of membrane contact sites. Biochimica et Biophysica Acta, 1833(11), 2526–2541.

Honigberh, B. M., King, V. M., 1964. Structure of *Trichomonas vaginalis* Donn'e. The Journal of Parasitology, 50, 345–364.

Hrdy, I., Hirt, R. P., Dolezal, P., Bardonová, L., Foster, P. G., Tachezy, J., Martin Embley, T., 2004. *Trichomonas* hydrogenosomes contain the NADH dehydrogenase module of mitochondrial complex I. Nature, 432(7017), 618–622.

Jedelsky, P. L., Bursac, D., Perry, A. J., Šedinová, M., Rada, P., Dolez, P., Smíšková, K., Novotný, M., Beltrán, N. C., Lithgow, T., Tachezy, J., 2011. The core components of organelle biogenesis and membrane transport in the hydrogenosomes of *Trichomonas vaginalis*. PLoS One, 6(9).

Jeong, H., Park, J., Jun, Y., Lee, C., 2017. Crystal structures of Mmm1 and Mdm12–Mmm1 reveal mechanistic insight into phospholipid trafficking at ER-mitochondria contact sites. Proceedings of the National Academy of Sciences, 114(45), 9502-9511.

Jeong, H., Park, J., Lee, C., 2016. Crystal structure of Mdm12 reveals the architecture and dynamic organization of the ERMES complex. EMBO Reports, 17(12), 1857-1871.

Kojima, R., Endo, T., Tamura, Y., 2016. A phospholipid transfer function of ER-mitochondria encounter structure revealed in vitro. Scientific Reports, 6, 30777.

Kornmann, B., Osman, C., Walter, P., 2011. The conserved GTPase Gem1 regulates endoplasmic reticulum-mitochondria connections. Proceedings of the National Academy of Sciences, 108(34), 14151–14156.

Kornmann, B., Walter, P., 2010. ERMES-mediated ER-mitochondria contacts: molecular hubs for the regulation of mitochondrial biology. Journal of Cell Science, 123(9), 1389-1393.

Kornmann, Benoît, Currie, E., Collins, S. R., Schuldiner, M., Nunnari, J., Weissman, J. S., Walter, P., 2009. An ER-mitochondria tethering complex revealed by a synthetic biology

screen. Science, 325(5939), 477–481.

Lev, S., 2010. Non-vesicular lipid transport by lipid-transfer proteins and beyond. Nature Reviews, Molecular Cell Biology, 11(10), 739–750.

Lindmark, D. G., Muller, M., 1973. Hydrogenosome, a cytoplasmic organelle of the anaerobic flagellate *Tritrichomonas foetus*, and its role in pyruvate metabolism. Journal of Biological Chemistry, 248(22), 7724–7728.

Lynes, E. M., Simmen, T., 2011. Urban planning of the endoplasmic reticulum (ER): How diverse mechanisms segregate the many functions of the ER. Biochimica et Biophysica Acta, 1813(10), 1893-1905.

Makki, A., Rada, P., Žárský, V., Kereïche, S., Kováčik, L., Novotný, M., Jores, T., Rapaport, D., Tachezy, J., 2019. Triplet-pore structure of a highly divergent TOM complex of hydrogenosomes in *Trichomonas vaginalis*. PLoS Biology, 17(1).

Marchi, S., Patergnani, S., Pinton, P., 2014. The endoplasmic reticulum-mitochondria connection: One touch, multiple functions. Biochimica et Biophysica Acta, 1837(4), 461–469.

Masuda, T., Tomita, M., Ishihama, Y., 2008. Phase transfer surfactant-aided trypsin digestion for membrane proteome analysis. Journal of Proteome Research, 7(2), 731–740.

Mentel, M., Zimorski, V., Haferkamp, P., Martin, W., Henze, K., 2008. Protein import into hydrogenosomes of *Trichomonas vaginalis* involves both N-terminal and internal targeting signals: A case study of thioredoxin reductases. Eukaryotic Cell, 7(10), 1750-1757.

Mirmonsef, P., Krass, L., Landay, A., Spear, G. T., 2012. The role of bacterial vaginosis and *Trichomonas* in HIV transmission across the female genital tract. Current HIV Research, 10(3), 202–210.

Miyakawa, I., Sando, N., Kawano, S., Nakamura, S., Kuroiwa, T., 1987. Isolation of morphologically intact mitochondrial nucleoids from the yeast, *Saccharomyces cerevisiae*.

Journal of Cell Science, 88(4), 431-439.

Mooberry, S. L., Tien, G., Hernandez, A. H., Plubrukarn, A., Davidson, B. S., 1999. Laulimalide and isolaulimalide, new paclitaxel-like microtubule- stabilizing agents. Cancer Research, 59(3), 653-660.

Nass, M. M. K., 1969. Mitochondrial DNA: I. Intramitochondrial distribution and structural relations of single- and double-length circular DNA. Journal of Molecular Biology, 42(3), 521–528.

New England Biolabs, 2019. Q5® Site-Directed Mutagenesis Kit.

Newman, L., Rowley, J., Vander Hoorn, S., Wijesooriya, N. S., Unemo, M., Low, N., Stevens, G., Gottlieb, S., Kiarie, J., Temmerman, M., 2015. Global estimates of the prevalence and incidence of four curable sexually transmitted infections in 2012 based on systematic review and global reporting. PLoS One, 10(12).

Nguyen, T. T., Lewandowska, A., Choi, J. Y., Markgraf, D. F., Junker, M., Bilgin, M., Ejsing, C. S., Voelker, D. R., Rapoport, T. A., Shaw, J. M., 2012. Gem1 and ERMES do not directly affect phosphatidylserine transport from ER to mitochondria or mitochondrial inheritance. Traffic, 16(6), 880-890.

Novick, P., Zerial, M., 1997. The diversity of Rab proteins in vesicle transport. Current Opinion in Cell Biology, 9(4), 496–504.

Ogden, R. C., Adams, D. A., 1987. Electrophoresis in agarose and acrylamide gels. Methods in Enzymology, 152, 61-87.

Palade, G., 1975. Intracellular aspects of the process of protein synthesis. Science, 189(4200), 347–358.

Petrin, D., Delgaty, K., Bhatt, R., Garber, G., 1998. Clinical and microbiological aspects of *Trichomonas vaginalis*. Clinical Microbiology Reviews, 11(2), 300–317.

Rabouille, C., 2014. Old dog, new tricks: Arf1 required for mitochondria homeostasis. The EMBO Journal, 33(22), 2604-2605.

Rada, P., Makki, A., Žárský, V., Tachezy, J., 2019. Targeting of tail-anchored proteins to *Trichomonas vaginalis* hydrogenosomes. Molecular Microbiology, 111(3), 588-603.

Rappsilber, J., Mann, M., Ishihama, Y., 2007. Protocol for micro-purification, enrichment, pre-fractionation and storage of peptides for proteomics using StageTips. Nature Protocols, 2(8), 1896–1906.

Reinisch, K. M., De Camilli, P., 2016. SMP-domain proteins at membrane contact sites: Structure and function. Biochimica et Biophysica Acta, 1861(8), 924-927.

Rowland, A. A., Voeltz, G. K., 2012. Endoplasmic reticulum–mitochondria contacts: function of the junction. Nature Reviews Molecular Cell Biology, 13, 607-625.

Schauder, C. M., Wu, X., Saheki, Y., Narayanaswamy, P., Torta, F., Wenk, M. R., De Camilli, P., Reinisch, K. M., 2014. Structure of a lipid-bound extended synaptotagmin indicates a role in lipid transfer. Nature, 510(7506), 552–555.

Skelton, N. J., Kördel, J., Akke, M., Forsén, S., Chazin, W. J., 1994. Signal transduction versus buffering activity in Ca(2+)-binding proteins. Nature Structural Biology, 1(4), 239–245.

Sogo, L. F., Yaffe, M. P., 1994. Regulation of mitochondrial morphology and inheritance by Mdm10p, a protein of the mitochondrial outer membrane. The Journal of Cell Biology, 126(6), 1361–1373.

Štáfková, J., Rada, P., Meloni, D., Žárský, V., Smutná, T., Zimmann, N., Harant, K., Pompach, P., Hrdý, I., Tachezy, J., 2018. Dynamic secretome of *Trichomonas vaginalis*: Case study of β-amylases. Molecular & Cellular Proteomics : MCP, 17(2), 304–320.

Stehling, O., Lill, R., 2013. The role of mitochondria in cellular iron-sulfur protein biogenesis: mechanisms, connected processes, and diseases. Cold Spring Harbor Perspectives in Biology, 5(8).

Tachezy, J., Doležal, P., 2007. Iron-sulfur proteins and iron-sulfur cluster assembly in organisms with hydrogenosomes and mitosomes. In Origin of Mitochondria and Hydrogenosomes, 105–133.

Tachezy, J., Sánchez, L. B., Müller, M., 2001. Mitochondrial type iron-sulfur cluster assembly in the amitochondriate eukaryotes *Trichomonas vaginalis* and *Giardia intestinalis*, as indicated by the phylogeny of IscS. Molecular Biology and Evolution, 18(10), 1919–1928.

Tamura, Y., Sesaki, H., Endo, T., 2014. Phospholipid transport via mitochondria. Traffic, 15(9), 933–945.

Toulmay, A., Prinz, W. A., 2012. A conserved membrane-binding domain targets proteins to organelle contact sites. Journal of Cell Science, 125(1), 49–58.

Vance, J. E., 1990. Phospholipid synthesis in a membrane fraction associated with mitochondria. Journal of Biological Chemistry, 265(13), 7248–7256.

Voss, C., Lahiri, S., Young, B. P., Loewen, C. J., Prinz, W. A., 2012. ER-shaping proteins facilitate lipid exchange between the ER and mitochondria in *S. cerevisiae*. Journal of Cell Science, 125(20), 4791–4799.

Wideman, J. G., Gawryluk, R. M. R., Gray, M. W., Dacks, J. B., 2013. The ancient and widespread nature of the ER-mitochondria encounter structure. Molecular Biology and Evolution, 30(9), 2044–2049.

Xue, Y., Schmollinger, S., Attar, N., Campos, O. A., Vogelauer, M., Carey, M. F., Merchant, S. S., Kurdistani, S. K., 2017. Endoplasmic reticulum–mitochondria junction is required for iron homeostasis. Journal of Biological Chemistry, 292(32), 13197-13204.

Youngman, M. J., Hobbs, A. E. A., Burgess, S. M., Srinivasan, M., Jensen, R. E., 2004. Mmm2p, a mitochondrial outer membrane protein required for yeast mitochondrial shape and maintenance of mtDNA nucleoids. Journal of Cell Biology, 164(5), 677–688.

Zhang, B., Yu, Q., Huo, D., Li, J., Liang, C., Li, H., Yi, X., Xiao, C., Zhang, D., Li, M., 2018.

Arf1 regulates the ER–mitochondria encounter structure (ERMES) in a reactive oxygen species-dependent manner. FEBS Journal, 258(11), 2004-2018.